IEEE Access
Multidisciplinary | Rapid Review | Open Access Journal

Received May 28, 2020, accepted June 27, 2020, date of publication July 2, 2020, date of current version July 15, 2020.

Digital Object Identifier 10.1109/ACCESS.2020.3006489

Fuzzy Observer-Based Dynamic Surface Control for Input-Saturated Nonlinear Systems and Its Application to Missile Guidance

WENGUANG ZHANG AND WENJUN YI
National Key Laboratory Transient Physics, Nanjing University of Science and Technology, Nanjing 210094, China
Corresponding author: Wenjun Yi (njustwz@163.com)

ABSTRACT In this paper, a fuzzy observer-based tracking control scheme is proposed for a class of strict-feedback uncertain nonlinear system with input saturation. To facilitate the fuzzy logic system (FLS) design, the original uncertain nonlinear system is transformed into an output feedback system firstly. Then, an adaptive state observer is constructed. In order to efficiently tackle the input saturation, an auxiliary system (AS) is introduced. Using the estimated states and AS, the dynamic surface control (DSC) strategy is developed based on backstepping method. Under the DSC scheme, the tracking control problem is reduced to optimal regulation problem of an affine system. Subsequently, an adaptive dynamic programming (ADP) based optimal control scheme is proposed. The stability of the overall system is guaranteed by Lyapunov theory. Finally, guidance simulation is made to confirm the effectiveness of the developed control method.

INDEX TERMS Adaptive dynamic programming, dynamic surface control, adaptive fuzzy control, input saturation, missile guidance systems.

I. INTRODUCTION

During the past two decades, adaptive control for nonlinear systems has attracted considerable attention and many important control schemes have been proposed and applied to the missile guidance systems [1]–[6]. These methods aim to increase the destructive power, or reduce the sensitivity to the target's maneuverability, or enhance the survivability of the missile. Besides, there are some optimal ones [7]–[11]. Such guidance laws can not only reduce the energy consumption in flight, but also constrain the miss distance. As the missiles are developed towards miniaturization, to study the guidance optimality is undoubtedly beneficial and necessary.

On the other hand, in order to make the designed guidance law play the expected effect in practical use, control saturation should be explicitly considered in the control design. Control saturation is caused by the physical limitation of actuator, and the control performance may degrade if this problem is neglected. In severe cases, it may even bring instability to the system [12]. Given this, many scholars have studied the design of guidance laws considering control saturation [13]–[16]. In [13], three dimensional guidance law for ground stationary target is investigated. To handle the control saturation, an auxiliary system is introduced. In order to deal with the maneuvering target, in [14], the authors utilize sliding mode control (SMC) and observer to design a guidance law with input constraint. In [15], input-to-state stability(ISS) theory is used to compensate the effect of control saturation and guarantee the system stability. In [16], an optimal control theory based guidance law is proposed. Because the control input, i.e., the acceleration command, has a profound effect on the homing performance, the authors also take this importance constraint into consideration. It should be noted that the guidance laws in [13]–[15] do not take any optimality into consideration. Although the guidance law in [16] is an optimal one, the proposed guidance law relies on a linearized model, which is based on small angle assumption. When such assumption is invalid, the system performance may be degraded. Therefore, to enhance the system stability, optimal guidance law based on nonlinear kinematic model while considering control saturation should be further developed.

As we know, dealing nonlinear optimal control problem requires solving the Hamilton-Jacobi-Bellman (HJB) equation. Although dynamic programming as an traditional method can solve optimal control problem, it suffers from

The associate editor coordinating the review of this manuscript and approving it for publication was Xiaosong Hu.

the curse of dimensionality. ADP can avoid this difficulty, and is widely used in nonlinear control design [17]–[20]. In [17], the HJB equation is solved by a novel adaptive value iteration method, where proper approximation error can be adaptively updated, such that the performance index can always converge. In [18], ADP method is applied to the optimal stabilization problem of a class of nonlinear system which contains uncertain dynamics and unknown orders. For model-free cases, in [19], recurrent neural network is used to construct system model based on input and output information, and ADP is utilized to derive an optimal controller. In [20], the tracking control problem of strict-feedback nonlinear system is investigated. The authors use backstepping technique to derive a feedforward controller, which can convert the tracking control problem into optimal regulation problem. Moreover, they further investigate the case of the system with unknown dynamics in [21]. Similar to [20], the work in [21] also uses backstepping method, which is an useful tool for nonlinear control design [22]–[26]. It is worth noting that there exists the problem of explosion of complexity for traditional backstepping method. DSC can effectively tackle this problem [27]. In [28], a high efficiency tracking control scheme for nonlinear systems based on DSC technique and a novel event-triggered mechanism is proposed. In [29], the problem of decentralized secure control for Cyber-physical systems (CPSs) in the presence of intermittent denial-of-service (Dos) and external disturbances is investigated. To reduce the computational burden, DSC method is also utilized in the design of control laws. Considering that the missile-target relative motion can be described by a strict-feedback uncertain nonlinear system, optimal tracking control design based on DSC technique for such system should be further investigated.

In practical engineering, plants with partially unmeasurable states are commonly seen [30], [31]. The missile guidance systems are no exception, such as the line-of-sight (LOS) rate cannot be measured directly. It is often obtained through filtering the output signals of a rate gyro which is mounted on the inner gimbal of the seeker. Therefore, the obtained LOS rate is vulnerable to time delays and noise. Besides, the gimballed seekers would squeeze into the warhead's already cramped space. For these reasons, some more practical guidance laws have been proposed [32], [33]. Despite the guidance law proposed in [32] owns the form of proportional navigation guidance, the generated guidance command does not contain LOS rate information. In [33] initial LOS rate information is needed to formulate the reference LOS rate profile, which is tracked by SMC based controller. However, neither of the two approaches consider any optimality.

Motivated by the aforementioned analysis, this paper proposes a tracking control scheme for a class of strict-feedback nonlinear system with unknown internal dynamics and partially unmeasurable states. We utilize FLS to approximate the internal dynamics. On this basis, an adaptive state observer is constructed. To explicitly tackle the control saturation issue, an AS is integrated. Using the estimated states and DSC method, we derive a novel feedforward controller, which reduces the tracking control problem to regulation issue. Subsequently, an FLS based optimal control strategy is introduced to estimate the value function. The estimated value function is then used to construct the optimal feedback controller. Finally, we analyze the stability of the overall system based on Lyapunov theory. Compared with the existing works, the main contributions of this paper can be summarized as follows:

1) Compared with [8], [11], [16], the optimal guidance law proposed in this paper does not need small angle assumption. Instead, it is totally based on missile-target nonlinear kinematic model. Therefore, the scheme presented in this paper can be applied to more complex cases.
2) Compared with [10], [20], this paper copes with input saturation issue explicitly, which makes the proposed method be more practical.
3) In this paper, the strict-feedback system is transformed into an output feedback system firstly, then an adaptive observer is constructed to estimate the states. Compared with [9], [20], [34], [35], this paper does not require the whole states of the system are measurable. For missile guidance systems, the benefit is that it can save space inside the warhead and be equipped with other advanced equipment to enhance the missile's power.
4) The stability of the whole system is analyzed with considering all the uncertainties and errors introduced, which is quite challenging.

The rest part of this paper is organized as follows: In Section II, we give some preliminaries and the problem to be studied. In Section III, an FLS based observer is constructed firstly, then DSC method is utilized to derive a feedforward controller. In Section IV, ADP is used to design the optimal controller. The stability analysis of the whole system is conducted in Section V. Simulation and results are given in Section VI. In Section VII, concluding remarks are presented.

II. PROBLEM STATEMENT AND PRELIMINARIES

A. PROBLEM STATEMENT

Consider a class of strict-feedback uncertain nonlinear system with partially unmeasurable states as follows:

$$\begin{aligned} \dot{x}_i &= f_i(\bar{x}) + g_i(\bar{x})x_{i+1}, \quad i = 1, 2, \ldots, n-1 \\ \dot{x}_n &= f_n(\bar{x}) + g_n(x_1)u(v(t)) \\ y &= x_1 \end{aligned} \tag{1}$$

where $\bar{x} = [x_1, x_2, \ldots, x_n]$, states x_i, $i = 2, \ldots, n$ are unmeasurable, $y \in \Re$ denotes system output; $f_i(\bar{x})$ are unknown smooth nonlinear functions; $u \in \Re$ denotes input, and is given by

$$u(v(t)) = sat(v(t)) = \begin{cases} u_M sign(v(t)), & |v(t)| \geq u_M \\ v(t), & otherwise \end{cases} \tag{2}$$

where u_M denotes the upper bound of $u(t)$. Control object of this paper is to design an adaptive optimal controller for system given in (1), such that the output y can track the reference signal y_d in an optimal manner.

Assumption 1 ([35]): Assume the control gain functions $g_i(\bar{x}) \neq 0$, and existing two constants which satisfy $0 < g_{min} < g_{max}$, such that $g_{min} < g_i(\bar{x}) < g_{max}$.

Assumption 2: Assume that y_d and its time derivative $\dot{y}_d$ satisfy $|y_d| < Y_0$, $|\dot{y}_d| < Y_1$, where Y_0 and Y_1 are two postive constants.

Assumption 3 ([36]): The plant is input-to-state stable (ISS).

Remark 1: Assumption 3 is reasonable due to the fact that a feasible control law which can globally stabilize an unstable plant in the presence of input saturation does not exist. For instance, consider a system $\dot{x} = \mathcal{A}x+u(v(t))$, where x denotes the state variable, and $u(v(t))$ is saturated input denoted by (2). If $\mathcal{A} > 0$ with the initial condition $x(0) > \frac{u_M}{\mathcal{A}}$, then, it is easy to verify that there does not exist any feasible control which satisfies (2) to stabilize the system; if $\mathcal{A} < 0$, a bounded input is capable to stabilize the above system. Therefore, Assumption 3 is needed to facilitate the stability analysis.

B. FUZZY LOGIC SYSTEMS

An FLS consists of a fuzzifier, knowledge base, fuzzy inference engine, and a defuzzifier. The knowledge base is comprised of a collection of fuzzy IF-THEN rules, which can be described as follows:

$$\begin{aligned} Rule^l : \text{IF } x_1 \text{ is } F_{l1}, x_2 \text{ is } F_{l2}, \ldots, x_n \text{ is } F_{ln}, \\ \text{THEN, } y \text{ is } G_l, l = 1, 2, \ldots, M \end{aligned} \tag{3}$$

where $x = (x_1, \ldots, x_n)$ and y represent FLS input and output. F_{li} are fuzzy sets, G_l denotes the output fuzzy singleton of the i rule,M denotes the quantity of rules in the knowledge base. The output of a FLS can be given by:

$$y(x) = \frac{\sum_{l=1}^{M} \bar{y}_l \left(\prod_{i=1}^{n} \mu_{F_{li}}(x_i) \right)}{\sum_{l=1}^{M} \left(\prod_{i=1}^{n} \mu_{F_{li}}(x_i) \right)} \tag{4}$$

where $\bar{y}_l = \max_{y \in R} \mu_{G_l}(y)$, $\mu_{F_{li}}(x_i)$ represents the degree of x_i in F_{li}. (4) can be rewritten as

$$y(x) = \theta^T \varphi(x) \tag{5}$$

where $\theta = [\bar{y}_1, \ldots, \bar{y}_M]^T$ is adjusable parameter vector, and $\varphi(x) = [\varphi_1(x), \ldots, \varphi_M(x)]^T$ denotes fuzzy basis function vector given by follows:

$$\varphi^l(x) = \frac{\prod_{i=1}^{n} \mu_{F_{li}}(x_i)}{\sum_{i=1}^{M} \left(\prod_{i=1}^{n} \mu_{F_{li}}(x_i) \right)} \tag{6}$$

III. PROBLEM TRANSFORMATION THROUGH ADAPTIVE DSC

In this section, to facilitate feedforward controller design in the existence of partially unmeasurable states, we firstly transform the original system into an output feedback system, then, an FLS based observer will be constructed to estimate the states. Subsequently, DSC technique is used to design a feedforward controller, which can convert the tracking control problem into optimal regulation issue.

A. SYSTEM TRANSFORMATION AND ADAPTIVE OBSERVER DESIGN

To facilitate the DSC design, we can transform the system denoted as (1) into an output feedback nonlinear system as follows [37]:

$$\begin{aligned} \dot{\xi}_i &= \xi_{i+1} + \Xi_i(y) \\ &\quad \text{for} \quad 1 \leq i \leq n-1 \\ \dot{\xi}_n &= \Xi_n(y) + \beta(y)u(v(t)) \end{aligned} \tag{7}$$

where $y = \xi_1 = x_1$. According to coordinate transformation, it is easy to verify that $\beta(y) = g_n(y)$.

Due to the universal approximate property of FLS, we can express the nonlinear functions Ξ_i as

$$\Xi_i(y) = \theta_i^{*T} \varphi(y) + \varepsilon_{i,\Xi} \tag{8}$$

where θ_i^{*T} and $\varphi(y)$ denotes ideal vector and fuzzy basis function, respectively. ε_{Ξ} is approximation error which satisfies $|\varepsilon_{i,\Xi}| \leq \delta_{i,M}$.

Since the states ξ_i, $i = 2, n$ can not be measured directly, it is essential to design an observer to reconstruct them. Therefore, a novel FLS based observer is proposed as:

$$\dot{\hat{\xi}} = A\hat{\xi} + k(y - \hat{y}) + \hat{\theta}\varphi(y) + b\beta(y)u(v(t)) \tag{9}$$

where

$$A = \begin{bmatrix} 0 & & I \\ \vdots & \ddots & \\ 0 & \cdots & 0 \end{bmatrix}, \quad b = \begin{bmatrix} 0 \\ \vdots \\ 0 \\ 1 \end{bmatrix}, \quad \hat{\theta} = \begin{bmatrix} \hat{\theta}_1^T \\ \hat{\theta}_2^T \\ \vdots \\ \hat{\theta}_n^T \end{bmatrix}, \quad k = \begin{bmatrix} k_1 \\ k_2 \\ \vdots \\ k_n \end{bmatrix},$$

with $\hat{\theta}_i$ representing the estimate of θ_i, and it satisfies $|\theta_i| \leq \theta_{i,M}$.

Note that $u(v(t))$ is segemented. A smooth function can be used to approximate it [33]:

$$h(v) = u_M \tanh(\frac{v}{u_M}) = u_M \frac{e^{v/u_M} - e^{-v/u_M}}{e^{v/u_M} + e^{-v/u_M}} \tag{10}$$

the approximation error $\Delta(v)$ satisfies

$$|\Delta(v)| = |(sat)(v) - h(v)| \leq u_M(1 - \tanh(1)) = \bar{d} \tag{11}$$

Thus, (9) changes into

$$\dot{\hat{\xi}} = A\hat{\xi} + k(y - \hat{y}) + \hat{\theta}\varphi(y) + b\beta(y)h(v) + D(t) \tag{12}$$

where $D(t) = b\beta(y)\Delta(v)$.

B. FEEDFORWARD CONTROLLER DESIGN

Based on (12), a feedforward controller is designed in this subsection. The detailed design process is given as follows.

Step 1: Denote the estimate tracking error as:

$$\hat{e}_1 = \hat{y} - y_d \tag{13}$$

Differetiating $\hat{e}_1$ with respect to time, one obtains

$$\begin{aligned}\dot{\hat{e}}_1 &= \dot{\hat{y}} - \dot{y}_d \\ &= \dot{\hat{\xi}}_1 - \dot{y}_d \\ &= \hat{\xi}_2 + k_1(y-\hat{y}) + \hat{\theta}_1\varphi(y) - \dot{y}_d \end{aligned} \tag{14}$$

Assume that $\xi_{id} = \xi_{id}^a + \xi_{id}^*$ are virtual inputs, with ξ_{id}^a denoting virtual feedforward controller, and ξ_{id}^* denoting optimal controller, which will be given in the next section. Choosing ξ_{2d}^a as

$$\xi_{2d}^a = \hat{f}_1 - \gamma_1\hat{e}_1 - k_1(y-\hat{y}) - \hat{\theta}_1^T\varphi(y) + \dot{y}_d \tag{15}$$

where $\hat{f}_1 = \hat{\theta}_1^T\varphi(e_1)$ with $\varphi(e_1) = \varphi(y) - \varphi(y_d)$. $k_1, \gamma_1 > 0$ are design parameters.

Introducing a first-order filter λ_2, and letting ξ_{2d} go through it with a time constant τ_2, yields

$$\tau_2\dot{\lambda}_2 + \lambda_2 = \xi_{2d}, \quad \lambda_2(0) = \xi_{2d}(0) \tag{16}$$

Denoting $\hat{e}_2 = \hat{\xi}_2 - \lambda_2$ and $\eta_2 = \lambda_2 - \xi_{2d}$, we have $\dot{\lambda}_2 = -\eta_2/\tau_2$ and $\hat{\xi}_2 = \hat{e}_2 + \eta_2 + \xi_{2d}$. Considering (15), (14) can be rewritten as

$$\dot{\hat{e}}_1 = \hat{e}_2 + \eta_2 + \hat{\xi}_{2d}^* + \hat{f}_1 - \gamma_1\hat{e}_1 \tag{17}$$

For η_2, the following inequality holds

$$\begin{aligned}\dot{\eta}_2 &= \dot{\lambda}_2 - \dot{\xi}_{2d} \\ &= -\frac{\eta_2}{\tau_2} + \Big(- \frac{\partial\xi_{2d}}{\partial\hat{\xi}_1}\dot{\hat{\xi}}_1 - \frac{\partial\xi_{2d}}{\partial\hat{e}_1}\dot{\hat{e}}_1 - \frac{\partial\xi_{2d}}{\partial\hat{\theta}_1}\dot{\hat{\theta}}_1 - \frac{\partial\xi_{2d}}{\partial y_d}\dot{y}_d\Big) \\ &= -\frac{\eta_2}{\tau_2} + N_2(\hat{e}_1, \hat{e}_2, \eta_2, \hat{\theta}_1, y_d, \dot{y}_d, \ddot{y}_d) \end{aligned} \tag{18}$$

where $N_2(\hat{e}_2, \hat{e}_2, \eta_2, \hat{\theta}_1, y_d, \dot{y}_d, \ddot{y}_d) = \Big(- \frac{\partial\xi_{2d}}{\partial\hat{\xi}_1}\dot{\hat{\xi}}_1 - \frac{\partial\xi_{2d}}{\partial\hat{e}_1}\dot{\hat{e}}_1 - \frac{\partial\xi_{2d}}{\partial\hat{\theta}_1}\dot{\hat{\theta}}_1 - \frac{\partial\xi_{2d}}{\partial y_d}\dot{y}_d\Big)$ is a continuous function. So, the boundedness of N_2 can be verified. According to [12], there exists a postive constant B_2, such that $|N_2| \le B_2$.

Considering the following Lyapunov function

$$V_1 = \frac{1}{2}\hat{e}_1^2 + \frac{1}{2}\eta_2^2 + \frac{1}{2}\widetilde{\xi}_1^2 + \frac{1}{2}\widetilde{\theta}_1^T\widetilde{\theta}_1 \tag{19}$$

where $\widetilde{\xi}_i = \xi_i - \hat{\xi}_i$ denotes state estimate error, $\widetilde{\theta}_i = \theta_i - \hat{\theta}_i$ denotes weight estimate error. Calculating the time derivative of V_1, yields

$$\begin{aligned}\dot{V}_1 = &-\gamma_1\hat{e}_1^2 + \hat{e}_1(\hat{h}_1(e_1) + \xi_{2d}^* + \hat{e}_2) \\ &+ \eta_2(-\frac{\eta_2}{\tau_2} + N_2) + \widetilde{\xi}_1\dot{\widetilde{\xi}}_1 + \widetilde{\theta}_1^T\dot{\widetilde{\theta}}_1 \end{aligned} \tag{20}$$

Using (12), the error dynamics of the observer can be given by

$$\dot{\widetilde{\xi}} = A\widetilde{\xi} - kc^T\widetilde{\xi} + \widetilde{\theta}^T\varphi(y) + \varepsilon_\Xi \tag{21}$$

where $c = [1, 0, \ldots, 0]^T$, $\varepsilon_\Xi = [\varepsilon_{1,\Xi}, \ldots, \varepsilon_{n,\Xi}]^T$. The update laws for θ_i are proposed as

$$\begin{aligned}\dot{\hat{\theta}}_i = &-\hat{e}_i(\varphi(y) - \varphi(y_d)) - \vartheta_i\hat{\theta}_i \parallel \varphi(y) \parallel^2 - \zeta_i\hat{\theta}_i \\ &- \iota_i\hat{\theta}_i(\hat{\theta}_i^T\hat{\theta}_i), \quad i = 1, \ldots, n \end{aligned} \tag{22}$$

where $\vartheta_i, \zeta_i, \iota_i > 0$ are design parameters.

Substituting (21) and (22) into (20), one obtains

$$\begin{aligned}\dot{V}_1 = &-\gamma_1\hat{e}_1^2 + \hat{e}_1(\hat{h}_1(e_1) + \widetilde{h}_1(e_1) + \xi_{2d}^* + \hat{e}_2 + \eta_2) \\ &+ \eta_2(-\frac{\eta_2}{\tau_2} + N_2) + \widetilde{\xi}_1\widetilde{\xi}_2 - k_1\widetilde{\xi}_1\widetilde{\xi}_1 + \widetilde{\theta}_1^T\varphi(y)\widetilde{\xi}_1 \\ &+ \varepsilon_{1,\Xi}\widetilde{\xi}_1 + \vartheta_1\widetilde{\theta}_1^T\hat{\theta}_1 \parallel \varphi(y) \parallel^2 + \zeta_1\widetilde{\theta}_1^T\hat{\theta}_1 \\ &+ \iota_1\widetilde{\theta}_1^T\hat{\theta}_1(\hat{\theta}_1^T\hat{\theta}_1) \end{aligned} \tag{23}$$

where $\widetilde{h}_1(e_1) = \widetilde{\theta}_1^T\varphi(e_1)$. Using Young's inequation, one can have

$$\widetilde{\theta}_1^T\varphi(y)\widetilde{\xi}_1 + \varepsilon_{1,\Xi}\widetilde{\xi}_1 \le \frac{1}{2} \parallel \widetilde{\theta}_1 \parallel^2 \parallel \varphi(y) \parallel^2 + \frac{1}{2}\varepsilon_{1,\Xi}^2 + \widetilde{\xi}_1^2 \tag{24}$$

Besides, we notice that

$$\begin{aligned}&\frac{1}{2} \parallel \widetilde{\theta}_1 \parallel^2 \parallel \varphi(y) \parallel^2 + \vartheta_1\widetilde{\theta}_1\hat{\theta}_1 \parallel \varphi(y) \parallel^2 \\ &\quad\le \Big(- (\vartheta_1 + \frac{1}{2}) \parallel \widetilde{\theta}_1 \parallel^2 + \parallel \widetilde{\theta}_1 \parallel \theta_{1,M}\Big) \parallel \varphi(y) \parallel^2 \\ &\quad\le \frac{\varphi_M^2\theta_{1,M}^2}{4(\vartheta_1 + \frac{1}{2})} \end{aligned} \tag{25}$$

where $\varphi_M = \max\{\|\varphi(y)\|\}$. On the other hand,

$$\begin{aligned}&\iota_1\widetilde{\theta}_1^T\hat{\theta}_1(\hat{\theta}_1^T\hat{\theta}_1) \\ &\quad= \big(\iota_1\widetilde{\theta}_1^T\theta_1 - \iota_1\widetilde{\theta}_1^T\widetilde{\theta}_1\big)\|\theta_1\|^2 \\ &\qquad- 2\iota_i(\widetilde{\theta}_i^T\theta_i)^2 + 3\iota_1\widetilde{\theta}_i^T\widetilde{\theta}_1(\widetilde{\theta}_1^T\theta_1) - \iota_1(\widetilde{\theta}_1^T\widetilde{\theta}_1)^2 \\ &\quad\le \iota_1\theta_{1,M}^3\|\widetilde{\theta}_1\| + 3\iota_1\theta_{1,M}\|\widetilde{\theta}_1\|^3 - \iota_1\|\widetilde{\theta}_1\|^4 \end{aligned} \tag{26}$$

Thus, (23) can be rewritten as

$$\begin{aligned}\dot{V}_1 \le &-\big(\gamma_1 - \frac{1}{2}\big)\hat{e}_1^2 + \hat{e}_1\Big(\hat{f}_1(e_1) + \widetilde{f}_1(e_1) \\ &+ \xi_{2d}^* + \hat{e}_2\Big) - \big(\frac{1}{\tau_2} - 1\big)\eta_2^2 + \frac{1}{2}B_2^2 + \widetilde{\xi}_1\widetilde{\xi}_2 \\ &- k_1\widetilde{\xi}_1^2 + \frac{1}{2}\varepsilon_{1,\Xi}^2 + \widetilde{\xi}_1^2 + \frac{\varphi_M^2\theta_{1,M}^2}{4(\eta_1 + \frac{1}{2})} + \big(\iota_1\theta_{1,M}^3 \\ &+ \zeta_1\theta_{1,M}\big)\|\widetilde{\theta}_1\| + 3\iota_1\theta_{1,M}\|\widetilde{\theta}_1\|^3 - \iota_1\|\widetilde{\theta}_1\|^4 \end{aligned} \tag{27}$$

Step i($2 \le i \le n-1$): In the ith step, we denote the estimate tracking error variable as

$$\hat{e}_i = \hat{\xi}_i - \lambda_i \tag{28}$$

Taking the time derivative of (28), yields

$$\begin{aligned}\dot{\hat{e}}_i &= \dot{\hat{\xi}}_i - \dot{\lambda}_i \\ &= \hat{e}_{i+1} + \xi_{(i+1)d}^a + \xi_{(i+1)d}^* + k_i(y-\hat{y}) + \hat{\theta}_i^T\varphi(y) \\ &\quad - \dot{\lambda}_i \end{aligned} \tag{29}$$

Choosing $\xi_{(i+1)d}^a$ as

$$\xi_{(i+1)d}^a = \hat{f}_i - \hat{e}_{i-1} - \gamma_i\hat{e}_i - k_i(y-\hat{y}) - \hat{\theta}_i^T\varphi(y) + \dot{\lambda}_i \tag{30}$$

Introducing a first-order filter λ_{i+1}, and letting $\xi_{(i+1)d}$ go through it with a time constant τ_{i+1}, yields

$$\tau_{i+1}\dot{\lambda}_{i+1} + \lambda_{i+1} = \xi_{(i+1)d}, \quad \lambda_{i+1}(0) = \xi_{(i+1)d}(0) \tag{31}$$

Denoting $\hat{e}_{i+1} = \hat{\xi}_{i+1} - \lambda_{i+1}$ and $\eta_{i+1} = \lambda_{i+1} - \xi_{(i+1)d}$, we have $\dot{\lambda}_{i+1} = -\eta_{i+1}/\tau_{i+1}$ and $\hat{\xi}_{i+1} = \hat{e}_{i+1} + \eta_{i+1} + \xi_{(i+1)d}$. On (30), (29) can be rewritten as

$$\dot{\hat{e}}_i = \hat{e}_{i+1} + \eta_{i+1} + \hat{\xi}^*_{(i+1)d} + \hat{h}_i - \gamma_i \hat{e}_i \tag{32}$$

For η_{i+1}, the following inequality holds

$$\begin{aligned}\dot{\eta}_{i+1} &= \dot{\lambda}_{i+1} - \dot{\xi}_{(i+1)d} \\ &= -\frac{\eta_{i+1}}{\tau_{i+1}} + \Big(- \frac{\partial \xi_{(i+1)d}}{\partial \hat{\xi}_i}\dot{\hat{\xi}}_i - \frac{\partial \xi_{(i+1)d}}{\partial \hat{e}_i}\dot{\hat{e}}_i \\ &\quad - \frac{\partial \xi_{(i+1)d}}{\partial \hat{\theta}_i}\dot{\hat{\theta}}_i - \frac{\partial \xi_{(i+1)d}}{\partial \lambda_i}\dot{\lambda}_i\Big) \\ &= -\frac{\eta_{i+1}}{\tau_{i+1}} + N_{i+1}(\hat{e}_i, \hat{e}_{i+1}, \eta_{i+1}, \hat{\theta}_i, \lambda_i, \dot{\lambda}_i, \ddot{\lambda}_i)\end{aligned} \tag{33}$$

where $N_{i+1}(\hat{e}_i, \hat{e}_{i+1}, \eta_{i+1}, \hat{\theta}_i, \lambda_i, \dot{\lambda}_i, \ddot{\lambda}_i) = \Big(- \frac{\partial \xi_{(i+1)d}}{\partial \hat{\xi}_i}\dot{\hat{\xi}}_1 - \frac{\partial \xi_{2d}}{\partial \hat{e}_1}\dot{\hat{e}}_1 - \frac{\partial \xi_{2d}}{\partial \hat{\theta}_i}\dot{\hat{\theta}}_i - \frac{\partial \xi_{(i+1)d}}{\partial \lambda_i}\dot{\lambda}_i\Big)$ is a continuous function. Therefore, the boundedness of N_{i+1} can be verified. According to [12], there exists a postive constant B_{i+1}, such that $|N_{i+1}| \le B_{i+1}$.

Consider the following Lyapunov function as

$$V_i = V_{i-1} + \frac{1}{2}\hat{e}_i^2 + \frac{1}{2}\eta_{i+1}^2 + \frac{1}{2}\widetilde{\xi}_i^2 + \frac{1}{2}\widetilde{\theta}_i^T\widetilde{\theta}_i \tag{34}$$

Taking the time derivative of (34), and using Young's inequality, one can obtain

$$\begin{aligned}\dot{V}_i &= \dot{V}_{i-1} - \gamma_i\hat{e}_i^2 + \hat{e}_i\Big(\hat{f}_i + \widetilde{f}_i + \xi^*_{(i+1)d} - \hat{e}_{i-1} + \hat{e}_{i+1} \\ &\quad + \eta_{i+1}\Big) + \eta_{i+1}(-\frac{\eta_{i+1}}{\tau_{i+1}} + N_{i+1}) + \widetilde{\xi}_i\widetilde{\xi}_{i+1} \\ &\quad - k_i\widetilde{\xi}_1\widetilde{\xi}_i + \widetilde{\theta}_i^T\varphi(y)\widetilde{\xi}_i + \varepsilon_{i,\Xi}\widetilde{\xi}_i + \vartheta_i\widetilde{\theta}_i^T\hat{\theta}_i \parallel \varphi(y) \parallel^2 \\ &\quad + \zeta_i\widetilde{\theta}_i^T\hat{\theta}_i + \iota_i\widetilde{\theta}_i^T\hat{\theta}_i\big(\hat{\theta}_i^T\hat{\theta}_i\big) \\ &\le -\sum_{j=1}^{i}\big(\gamma_j - \frac{1}{2}\big)\hat{e}_j^2 + \sum_{j=1}^{i}\hat{e}_j(\hat{f}_j + \widetilde{f}_j + \xi^*_{(j+1)d}) \\ &\quad + \hat{e}_i\hat{e}_{i+1} - \sum_{j=1}^{i}(\frac{1}{\tau_{i+1}} - 1)\eta_{i+1}^2 + \frac{1}{2}\sum_{j=1}^{i}B_{i+1}^2 \\ &\quad + \sum_{j=1}^{i}\widetilde{\xi}_j\widetilde{\xi}_{j+1} - \sum_{j=1}^{i}k_j\widetilde{\xi}_1\widetilde{\xi}_j + \sum_{j=1}^{i}\frac{1}{2}\varepsilon_{j,\Xi}^2 + \sum_{j=1}^{i}\widetilde{\xi}_j^2 \\ &\quad + \sum_{j=1}^{i}\frac{\varphi_M^2\theta_{j,M}^2}{4(\vartheta_j + \frac{1}{2})} + 3\sum_{j=1}^{i}\iota_j\theta_{j,M}\|\widetilde{\theta}_j\|^3 + \sum_{j=1}^{i}\big(\iota_j\theta_{j,M}^3 \\ &\quad + \zeta_j\theta_{j,M}\big)\|\widetilde{\theta}_j\| - \sum_{j=1}^{i}\iota_j\|\widetilde{\theta}_j\|^4\end{aligned} \tag{35}$$

Step n: In this step, denoting the estimate tracking error as:

$$\hat{e}_n = \hat{\xi}_n - \lambda_n - \varrho \tag{36}$$

where the auxilliary control signal ϱ is used to deal with input saturation problem.

Taking the time derivative of (36), yields

$$\begin{aligned}\dot{\hat{e}}_n &= \dot{\hat{\xi}}_n - \dot{\lambda}_{n+1} - \dot{\varrho} \\ &= k_n(y - \hat{y}) + \hat{\theta}_n\varphi(y) + \beta(y)h(v) + D(t) \\ &\quad - \dot{\lambda}_n - \dot{\varrho}\end{aligned} \tag{37}$$

Denoting the auxilliary system as

$$\dot{\varrho} = -l\varrho + \beta(y)(h(v(t)) - v(t)) \tag{38}$$

Choosing v_d^a as

$$\begin{aligned}v_d^a = \beta^{-1}\big(&\hat{f}_n - \hat{e}_{n-1} - (\gamma_n - \frac{1}{2})\hat{e}_n - k_n(y - \hat{y}) \\ &- \hat{\theta}_n^T\varphi(y) + \dot{\lambda}_n - l\varrho\big)\end{aligned} \tag{39}$$

Substituting (39) into (37), one obtains

$$\dot{\hat{e}}_n = \hat{f}_n - \hat{e}_{n-1} - \gamma_n\hat{e}_n + \bar{\beta}v_d^* + D(t) \tag{40}$$

Considering the following Lyapunov function

$$V_n = V_{n-1} + \frac{1}{2}\hat{e}_n^2 + \frac{1}{2}\widetilde{\xi}_n^2 + \frac{1}{2}\widetilde{\theta}_n^T\widetilde{\theta}_n \tag{41}$$

Taking the time derivative of (41), and using Young's inequality, one can obtain

$$\begin{aligned}\dot{V}_n &= \dot{V}_{n-1} - (\gamma_n - \frac{1}{2})\hat{e}_n^2 + \hat{e}_n\Big(\hat{f}_n + \widetilde{f}_n + v_d^* - \hat{e}_{n-1}\Big) \\ &\quad - k_n\widetilde{\xi}_1\widetilde{\xi}_n + \widetilde{\theta}_n^T\varphi(y)\widetilde{\xi}_n + \varepsilon_{n,\Xi}\widetilde{\xi}_n + \vartheta_n\widetilde{\theta}_n^T\hat{\theta}_n \parallel \varphi(y) \parallel^2 \\ &\quad + \zeta_n\widetilde{\theta}_n^T\hat{\theta}_n + \iota_n\widetilde{\theta}_n^T\hat{\theta}_n\big(\hat{\theta}_n^T\hat{\theta}_n\big) + \frac{1}{2} \parallel D(t) \parallel^2 \\ &\le -\sum_{j=1}^{n}(\gamma_j - \frac{1}{2})\hat{e}_j^2 - \sum_{j=2}^{n-1}(\frac{1}{\tau_i} - 1)\eta_i^2 + \frac{1}{2}\sum_{i=2}^{n-1}B_i^2 \\ &\quad + \widetilde{\xi}^T A_o\widetilde{\xi} + \sum_{j=1}^{n}\frac{1}{2}\varepsilon_{j,\Xi}^2 + \sum_{j=1}^{n}\frac{\varphi_M^2\theta_{j,M}^2}{4(\vartheta_j + \frac{1}{2})} - \sum_{j=1}^{n}\iota_i\|\widetilde{\theta}_i\|^4 \\ &\quad + \sum_{j=1}^{n}\big(\iota_i\theta_{i,M}^3 + \zeta_i\theta_{i,M}\big)\|\widetilde{\theta}_i\| + 3\sum_{j=1}^{n}\iota_i\theta_{i,M}\|\widetilde{\theta}_i\|^3 \\ &\quad + \frac{1}{2}g_{max}^2\bar{d}^2 \\ &\quad + \hat{E}^T\left(\begin{bmatrix}\hat{f}_1 \\ \vdots \\ \hat{f}_n\end{bmatrix} + \begin{bmatrix}\widetilde{f}_1 \\ \vdots \\ \widetilde{f}_n\end{bmatrix} + \begin{bmatrix}I_{n-1} & 0 \\ 0 & \beta(y)\end{bmatrix}\begin{bmatrix}\xi^*_{2d} \\ \vdots \\ \xi^*_{Nd} \\ v^*(t)\end{bmatrix}\right)\end{aligned} \tag{42}$$

where $\hat{E} = [\hat{e}_1, \hat{e}_2, \ldots, \hat{e}_n]^T$, $A_o = A - k + I_n$, and $U^* = [\xi^*_{2d}, \ldots, \xi^*_{nd}, v^*(t)]^T$.

At this point, we have finished the feedforward controller design. As mentioned above, the proposed controller consists of a feedforward controller and an optimal controller, and it can be given by $U = U^a + U^*$, where $U^a = [\xi^a_{2d}, \ldots, \xi^a_{nd}, v^a(t)]^T$. Note that in (42), if let $U^* = 0$ for $t > 0$, the tracking system will not be stable. In other words,

the proposed U^a transforms the tracking control problem to be studied into stabilization problem of the following system in affine form:

$$\dot{\hat{E}} = \hat{F} + \widetilde{F} + GU^* \tag{43}$$

where $G = \begin{bmatrix} I_{n-1} & 0 \\ 0 & \beta(y) \end{bmatrix}$, $\hat{F} = [\hat{f}_1, \ldots, \hat{f}_n]^T$, $\widetilde{F} = [\widetilde{f}_1, \ldots, \widetilde{f}_n]^T$. In the following section, we will design a feedback controller based on ADP technique. The controller can stabilize the system (43) in an optimal manner, and guarantees the stability of the whole closed-loop system.

IV. ADAPTIVE OPTIMAL CONTROLLER DESIGN

Consider the following nonlinear system

$$\dot{\hat{E}} = F + GU^* \tag{44}$$

where $F = \hat{F} + \widetilde{F}$. The corresponding cost function can be constructed as

$$V = \int_t^{\infty} Q(E) + U^{*T} R U^* d\tau \tag{45}$$

where $Q(E)$ denotes a postive semidefinite penalty function on states, R is a postive definite matrix. Next, we can obtain a Hamiltonian as

$$H = Q + U^{*T} R U^* + (\nabla V)^T (F + GU^*) \tag{46}$$

where $\nabla V = \partial V / \partial \hat{E}$. By solving the stationary condition $\partial H(\hat{E}, U^*)/\partial U^* = 0$, one can obtain the optimal control law as follows

$$U^* = -R^{-1} G^T \nabla V / 2 \tag{47}$$

Based on (46) and (47), HJB equation and the necessary and sufficient conditions of optimal control are given by

$$Q(\hat{E}) + (\nabla V)^{*T} \hat{F} - (\nabla V)^{*T} G R^{-1} G^T \nabla V^* / 4 = 0 \tag{48}$$

with $V^*(0) = 0$.

According to [35], we assume that the optimal system dynamics satisfy

$$\| F + GU^* \| \le \delta(\hat{E}) = \sqrt[4]{K \| \nabla J(\hat{E}) \|} \tag{49}$$

where $\delta(\hat{Z})$ is a function of system states, K is a postive constant, and $J(\hat{E})$ is a continuous differetiable Lyapunov candidate, which satisfies $\dot{J}(\hat{E}) = (\nabla J)^T \dot{\hat{E}} = (\nabla J)^T (F + GU^*) \le 0$. What's more, it can be shown that there exists a postive definite matrix $\bar{P}(\hat{E}) \in \Re^{n \times n}$, which leads

$$(\nabla J)^T (F + GU^*) = -(\nabla J)^T \bar{P} (\nabla J) \tag{50}$$

According to the universal approximate property, we can express the cost function as

$$V = W^T \phi(\hat{E}) + \varepsilon(\hat{E}) \tag{51}$$

where W is optimal vector, $\phi(\hat{E})$ is fuzzy basis vector, and $\varepsilon(\hat{E})$ is approximation error. Assume that the optimal vector and approximation error are upper bounded, such that $\| W \| \le W_M, \| \phi(\hat{E}) \| \le \phi_M$. According to [30], we can also assume that the gradient of approximation error along $\hat{E}$ is upper bounded, such that $\| \nabla \phi \| \le \phi'_M$.

Thus, the gradient of cost function can be given by

$$\partial V / \partial \hat{E} = \nabla V = W^T \nabla \phi(\hat{E}) + \nabla \varepsilon \tag{52}$$

Using (52), HJB equation (46) and the optimal control law (47) can be rewritten as

$$U^* = -R^{-1} G^T \nabla^T \phi(\hat{E}) W / 2 - R^{-1} G^T \nabla^T \epsilon / 2 \tag{53}$$

$$H^*(\hat{E}, \hat{W}) = Q + \hat{W}^T \nabla \phi(\hat{E}) F - W^T \nabla \phi(\hat{E}) D \nabla^T \phi(\hat{E}) W / 4 + \epsilon_{HJB} \tag{54}$$

where $D = GR^{-1}G^T > 0$ is bounded, such that $D_{min} \le \|D\| \le D_{max}$ for known constants D_{min} and D_{max}. The residual error $\varepsilon_{HJB} = \nabla^T \varepsilon \big[F - D\big(\nabla \phi(\hat{E}) W + \nabla \varepsilon\big)\big]/2 + \nabla^T \varepsilon D \nabla \varepsilon = \nabla^T \varepsilon (F + GU^*) + \nabla^T \varepsilon D \nabla \varepsilon / 4$. Considering the boundedness of the gradient of ε, and using (49), yields

$$\| \varepsilon_{HJB} \| \le \varepsilon'_M \delta(\hat{E}) + \varepsilon'^2_M D_{max} / 4 \tag{55}$$

Moving on, the estimate of V can be expressed as

$$\hat{V} = \hat{W}^T \phi(\hat{E}) \tag{56}$$

where $\hat{W}$ denotes the estimate of W. Similar, we can express the estimate optimal control law as

$$\hat{U}^* = -R^{-1} G^T \nabla^T \phi(\hat{E}) \hat{W} / 2 \tag{57}$$

On (56) and (57), Hamiltonian can be approximated as

$$\hat{H}^*(\hat{E}, \hat{W}) = Q + \hat{W}^T \nabla \phi(\hat{E}) \hat{F} - \hat{W}^T \nabla \phi(\hat{E}) D \nabla^T \phi(\hat{E}) \hat{W} / 4 = e_c \tag{58}$$

To obtain the update law of $\hat{W}$, we define an object function as

$$E_c = \frac{1}{2} e_c^T e_c \tag{59}$$

During the control process, the update law of $\hat{W}$ should not only be able to minimize E_c, but also can guarantee the stability of the overall system. To this end, the update law of $\hat{W}$ is formulated as

$$\dot{\hat{W}} = -\frac{\alpha_1 \hat{\sigma}}{\rho^2} e_c + \frac{\alpha_1}{2} \sum(\hat{E}, \hat{U}^*) \nabla \phi(\hat{E}) D \nabla^T \phi(\hat{E}) \nabla J \tag{60}$$

where $\hat{\sigma} = \nabla \phi(\hat{E})(\hat{F} + G\hat{U}^*)$, $\rho = (1 + \hat{\sigma}^T \hat{\sigma})$,$\alpha_1 > 0$ is design parameter, and the term $\sum(\hat{E}, \hat{U}^*)$ is given by

$$\sum(\hat{E}, \hat{U}^*) = \begin{cases} 0 & \text{if } \dot{J}(\hat{E}) < 0 \\ 1 & \text{otherwise} \end{cases} \tag{61}$$

Remark 2: For the FLS weight update law (60), the first term is used to minimize (59), and it is derived according to gradient descent algorithm. The second term is used to guarantee the system stability during control process.

Next, denoting the estimation error of W as $\widetilde{W}$,which satisfies $\widetilde{W} = W - \hat{W}$. Noting that

$$Q(\hat{E}) = -W^T\nabla\phi(\hat{E})F + W^T\nabla\phi(\hat{E})D\nabla^T\phi(\hat{E})W/4 - \varepsilon_{HJB} \quad (62)$$

and substituting (62) into (58), one can obtain

$$\begin{aligned}\hat{H}^*(\hat{E},\hat{W}) = &-\widetilde{W}^T\nabla\phi(\hat{E})\hat{F}(\hat{E}) - W^T\nabla\phi(\hat{E})\widetilde{F}(\hat{E}) \\ &+\frac{1}{2}W^T\nabla\phi(\hat{E})D\nabla^T\phi(\hat{E})\widetilde{W} \\ &-\frac{1}{4}\widetilde{W}^T\nabla\phi(\hat{E})D\nabla\phi^T(\hat{E})\widetilde{W} - \varepsilon_{HJB}\end{aligned} \quad (63)$$

Using (63), and observing that $\dot{\widetilde{W}} = -\dot{\hat{W}}$ and $\hat{\sigma} = \nabla\phi(\hat{E})(\dot{\hat{E}} + D\nabla\varepsilon/2) - \nabla\phi(\hat{E})\widetilde{F} + \nabla\phi(\hat{E})D\nabla^T\phi(\hat{E})\widetilde{W}/2$, one can obtain the error dynamics of (60) as

$$\begin{aligned}\dot{\widetilde{W}} = &-\frac{\alpha_1\hat{\sigma}}{\rho^2}\Big[\widetilde{W}^T\nabla\phi(\hat{E})\big(\dot{\hat{E}}^* + D\nabla^T\varepsilon/2\big) + \widetilde{W}^T \\ &\times\nabla\phi(\hat{E})\widetilde{F} - W^T\nabla\phi(\hat{E})\widetilde{F}\Big] - \frac{1}{4}\frac{\alpha_1\hat{\sigma}}{\rho^2}\Big(\widetilde{W}^T \\ &\times\nabla\phi(\hat{E})D\nabla^T\phi(\hat{E})\widetilde{W} + \varepsilon_{HJB}\Big) - \frac{\alpha_1}{2}\sum(\hat{E},\hat{U}^*) \\ &\times\nabla\phi(\hat{E})D\nabla\phi^T(\hat{E})\nabla J\end{aligned} \quad (64)$$

which will be used in stability analysis.

Remark 3: Noting that (64) contains the term of $\widetilde{F}$, which is different from [20], [35], [38]. On the one hand, this makes the stability analysis be more challenging; On the other hand, it increases the complexity of the FLS of the adaptive observer.

V. STABILITY ANALYSIS

In this section, we utilize the Lyapunov theory to analyze the stability of closed-loop system.

Theorem 1: For the nonlinear system given by (1) and its transforming system (7), if the state observer is designed as (12), the update laws of the corresponding FLS are designed as (22), the feedforward controllers are designed as (15),(30) and (39), and the optimal controller is designed as (57), the corresponding adaption law is given by (60), and the control parameters are properly selected, then, all of the signals will be uniformly ultimately bounded (UUB).

Proof: Considering the following Lyapunov function as

$$V_{HJB} = \frac{1}{2}\sum_{i=1}^{n}\hat{e}_i^2 + \frac{1}{2}\sum_{i=2}^{n}\hat{\eta}_i^2 + \alpha_2 J(\hat{E}) + \frac{\alpha_1^{-1}}{2}\widetilde{W}^T\widetilde{W} + \frac{1}{2}\widetilde{\xi}^T\widetilde{\xi} + \frac{1}{2}tr\big(\widetilde{\theta}^T\widetilde{\theta}\big) \quad (65)$$

where $J(\hat{E})$ is chosen to satisfy $J(\hat{E}) = (\hat{E}^T\hat{E})^{\frac{3}{2}}/3$. Taking the time derivative of (65), yields

$$\dot{V}_{HJB} = \sum_{i=1}^{n}\hat{e}_i\dot{\hat{e}}_i + \sum_{i=2}^{n-1}\hat{\eta}_i\dot{\hat{\eta}}_i + \alpha_2\nabla J^T\dot{\hat{E}} + \alpha_1^{-1}\widetilde{W}^T\dot{\widetilde{W}} + \widetilde{\xi}^T\dot{\widetilde{\xi}} + tr\big(\widetilde{\theta}^T\dot{\widetilde{\theta}}\big) \quad (66)$$

Recalling (42) and (64), one can obtain

$$\begin{aligned}\dot{V}_{HJB} \le &-\gamma_{min}\parallel\hat{E}\parallel^2 + \hat{E}(F + GU^*) + \alpha_2\nabla J^T\dot{\hat{E}} \\ &-\Big[\widetilde{W}^T\nabla\phi(\hat{E})\big(\dot{\hat{E}}^* + D\nabla\varepsilon/2\big)\Big]^2/\rho^2 - \frac{3}{8}\widetilde{W}^T \\ &\times\nabla\phi(\hat{E})\big(\dot{\hat{E}}^* + D\nabla\varepsilon/2\big)\widetilde{W}^T\nabla\phi(\hat{E})D\nabla^T\phi(\hat{E}) \\ &\times\widetilde{W}/\rho^2 - \frac{1}{8}\Big(\widetilde{W}^T\nabla\phi(\hat{E})D\nabla^T\phi(\hat{E})\widetilde{W}\Big)^2/\rho^2 \\ &-\widetilde{W}^T\nabla_{\hat{E}}\phi(\hat{E})(\dot{\hat{E}}^* + GU^*)W^T\nabla\phi(\hat{E})\widetilde{F}/\rho^2 \\ &-\frac{1}{4}\widetilde{W}^T\nabla_{\hat{E}}\phi(\hat{E})D\nabla^T\phi(\hat{E})\widetilde{W}\widetilde{W}^T\nabla\phi(\hat{E})\widetilde{F}/\rho^2 \\ &+\frac{1}{2}\widetilde{W}^T\nabla\phi(\hat{E})D\nabla^T\phi(\hat{E})\widetilde{W}W^T\nabla\phi(\hat{E})\widetilde{F}/\rho^2 \\ &-\frac{1}{4}\widetilde{W}\Big(\nabla\phi(\hat{E})(\dot{\hat{E}}^* + D\nabla\varepsilon/2\big) - \Big(\widetilde{W}^T\nabla\phi(\hat{E}) \\ &\times\widetilde{F}\Big)^2/\rho^2 + \widetilde{W}^T\nabla\phi(\hat{E})\widetilde{F}W^T\nabla\phi(\hat{E})\widetilde{F} \\ &+\frac{1}{2}\nabla\phi(\hat{E})D\nabla_{\hat{E}}^T\phi(\hat{E})\widetilde{W}\varepsilon_{HJB}/\rho^2 - \frac{1}{2}\widetilde{W}^T \\ &\times\sum(\hat{E},\hat{U}^*)\nabla_{\hat{E}}\phi(\hat{E})D\nabla\phi^T(\hat{E})\nabla J(\hat{E}) + \widetilde{\xi}^TA\widetilde{\xi} \\ &-\widetilde{\xi}^Tkc^T\widetilde{\xi} + \widetilde{\xi}^T\widetilde{\theta}\varphi(y) + \widetilde{\xi}\varepsilon_\Xi + \sum_{i=1}^{n}\zeta_i\widetilde{\theta}_i^T\hat{\theta}_i \\ &+\sum_{i=1}^{n}\vartheta_i\widetilde{\theta}_i^T\hat{\theta}_i\varphi^T(y)\varphi(y) + \sum_{i=1}^{n}\iota_i\widetilde{\theta}_i^T\hat{\theta}_i(\hat{\theta}_i^T\hat{\theta}_i) \\ &-\sum_{j=2}^{n-1}(\frac{1}{\tau_i} - 1)\eta_i^2 + \frac{1}{2}\sum_{i=2}^{n-1}B_i^2\end{aligned} \quad (67)$$

where γ_{min}=min$\{\gamma_1 - \frac{1}{2},\ldots,\gamma_n - \frac{1}{2}\}$. Applying Young's inequality and completing the squares, (67)can be rewritten as

$$\begin{aligned}\dot{V}_{HJB} \le &-\gamma_{min}\parallel\hat{E}\parallel^2 + \hat{E}(F + GU^*) + \alpha_2\nabla J^T\dot{\hat{E}} \\ &-\frac{752}{1152}\|\widetilde{W}\|^4\nabla\phi_{min}^4/\rho^2 + \Big(\frac{17}{8D_{min}^2} + \frac{5}{4}\Big)\delta^4(\hat{E})/\rho^2 \\ &+\frac{4}{17}\|\widetilde{F}\|^4/\rho^2 + \frac{5}{4}D_{min}^2\varepsilon_M'4W_M^4/\rho^2 \\ &+\frac{17}{16}D_{max}^2\varepsilon_M'^4 + \frac{5}{4}\big(\varepsilon_M'^4 + \varepsilon_M'^4D_{max}^2\big) + \frac{1}{2}\parallel\varepsilon_\Xi\parallel^2 \\ &+\frac{1}{2}\sum_{i=1}^{n}\theta_{i,M}^2 + ((A - kc^T)_{max} + 1)\|\widetilde{\xi}\|^2 \\ &-\sum_{i=1}^{n}(\vartheta_i - \frac{1}{2})\|\widetilde{\theta}_i\|^2\varphi^T(y)\varphi(y) - \sum_{i=1}^{n}\frac{1}{2}\zeta_i\|\widetilde{\theta}_i\|^2 \\ &+\sum_{i=1}^{n}\eta_i\theta_{i,M}\|\widetilde{\theta}_i\|\varphi^T(y)\varphi(y) + \sum_{i=1}^{n}\iota_i\widetilde{\theta}_i^T\hat{\theta}_i(\hat{\theta}_i^T\hat{\theta}_i) \\ &-\frac{1}{2}\widetilde{W}^T\sum(\hat{E},\hat{U}^*)\nabla\phi(\hat{E})D\nabla\phi^T(\hat{E})\nabla J(\hat{E}) \\ &-\sum_{j=2}^{n-1}(\frac{1}{\tau_i} - 1)\eta_i^2 + \frac{1}{2}\sum_{i=2}^{n-1}B_i^2\end{aligned} \quad (68)$$

where (49)and (55) are used, and $(A-kc^T)_{max}$ denotes the maximal eigenvalue of the matrix $(A-kc^T)$.

Note that $\|\widetilde{F}\|^4$ satisfies

$$\|\widetilde{F}\|^4 = \|\widetilde{\theta}\varphi(e_1)\|^4 = \Big(\sum_{i=1}^{n}\big(\widetilde{\theta}_i^T\varphi(e_1)\big)^2\Big)^2 \le n\bar{\varphi}_M^4\sum_{i=1}^{n}\|\widetilde{\theta}_i\|^4 \tag{69}$$

where Cauchy Schwarz inequality is used, and $\bar{\varphi}_M = \max\{\|\varphi_i(e_1)\|\}, i=1,\ldots,n$. Besides, the term $\sum_{i=1}^{n}\iota_i\widetilde{\theta}_i^T\hat{\theta}_i(\hat{\theta}_i^T\hat{\theta}_i)$ satisfies

$$\begin{aligned}&\sum_{i=1}^{n}\iota_i\widetilde{\theta}_i^T\hat{\theta}_i(\hat{\theta}_i^T\hat{\theta}_i)\\ &=\sum_{i=1}^{n}\iota_i\widetilde{\theta}_i^T\theta_i(\theta_i^T\theta_i)-\sum_{i=1}^{n}3\iota_i(\widetilde{\theta}_i^T\theta_i)^2\\ &\quad-\sum_{i=1}^{n}\iota_i(\widetilde{\theta}_i^T\widetilde{\theta}_i)^2+\sum_{i=1}^{n}3\iota_i\widetilde{\theta}_i^T\widetilde{\theta}_i(\widetilde{\theta}_i^T\theta_i)\\ &\le\sum_{i=1}^{n}\iota_i\theta_{i,M}^3\|\widetilde{\theta}_i\|+3\sum_{i=1}^{n}\iota_i\theta_{i,M}\|\widetilde{\theta}_i\|^3\\ &\quad-\sum_{i=1}^{n}\iota_i\|\widetilde{\theta}_i\|^4\end{aligned} \tag{70}$$

thus

$$\begin{aligned}&-\sum_{i=1}^{n}\frac{1}{4}\zeta_i\|\widetilde{\theta}_i\|^2+\sum_{i=1}^{n}\iota_i\widetilde{\theta}_i^T\hat{\theta}_i(\hat{\theta}_i^T\hat{\theta}_i)+\frac{4}{17}\|\widetilde{F}\|^4/\rho^2\\ &\le\sum_{i=1}^{n}\frac{1}{2}\iota_i\theta_{i,M}^6+\sum_{i=1}^{n}\Big(\big(-\frac{1}{4}\zeta_i+\frac{1}{2}\iota_i\big)\|\widetilde{\theta}_i\|^2\\ &\quad+3\iota_i\theta_{i,M}\|\widetilde{\theta}_i\|^3-\big(\iota_i-\frac{4n\bar{\varphi}_M^4}{17\rho^2}\big)\|\widetilde{\theta}_i\|^4\Big)\end{aligned} \tag{71}$$

In (67), to leads the second term

$$\sum_{i=1}^{n}\Big(\big(-\frac{1}{4}\zeta_i+\frac{1}{2}\iota_i\big)\|\widetilde{\theta}_i\|^2+3\iota_i\theta_{i,M}\|\widetilde{\theta}_i\|^3-(\iota_i-\frac{4n\bar{\varphi}_M^4}{17\rho^2})\|\widetilde{\theta}_i\|^4\Big)\le 0 \tag{72}$$

the design parameters ι_i and ζ_i should be selected to make the following inequality hold

$$\begin{cases}9\iota_i^2\theta_{i,M}^2-2(\iota_i-\frac{4n\bar{\varphi}_M^4}{17\rho^2})(\frac{1}{4}\zeta_i-\frac{1}{2}\iota_i)<0\\ \iota_i-\frac{4n\bar{\varphi}_M^4}{17\rho^2}>0\\ \frac{1}{2}\zeta_i-\iota_i>0\end{cases} \tag{73}$$

On (49), (68), (71) and (72), with noticing that $1/\rho^2\le 1$, the following inequality holds

$$\begin{aligned}\dot{V}_{HJB}\le&-\big(\gamma_{min}-\frac{1}{2}\big)\|\hat{E}\|^2+\frac{\sqrt{K}}{2}\|\hat{E}\|+\alpha_2\nabla J^T\dot{\hat{E}}\\ &+\beta_1\|\nabla J\|-\beta_2\|\widetilde{W}\|^4/\rho^2-\beta_3\|\widetilde{\xi}\|^2-\frac{1}{4}\sum_{i=1}^{n}\zeta_i\|\widetilde{\theta}_i\|^2\\ &+\sum_{i=1}^{n}\Big\{\underbrace{\Big[-(\vartheta_i-\frac{1}{2})\|\widetilde{\theta}_i\|^2+\eta_i\theta_{i,M}\|\widetilde{\theta}_i\|\Big]}_{\le\frac{(\vartheta_i\theta_{i,M})^2}{4(\vartheta_i-\frac{1}{2})}}\|\varphi(y)\|^2\Big\}\\ &-\frac{1}{2}\widetilde{W}^T\sum(\hat{E},\hat{U}^*)\nabla_{\hat{E}}\phi(\hat{E})D\nabla\phi^T(\hat{E})\nabla J+\beta_4\\ &-\sum_{j=2}^{n-1}(\frac{1}{\tau_i}-1)\eta_i^2\end{aligned} \tag{74}$$

where $\beta_1=\frac{17}{8D_{min}^2}K+\frac{5}{4}K,\beta_2=\frac{752}{1152}\nabla^4\phi_{min},\beta_3=-((A-kc^T)_{max}+1)$, and $\beta_4=\frac{5}{4}(\varepsilon_M'^4+\varepsilon_M'^4D_{max}^2)+\frac{n}{2}\bar{\varepsilon}_{\Xi M}^2+\frac{1}{2}\sum_{i=1}^{n}\theta_{i,M}^2+\sum_{i=1}^{n}\frac{1}{2}\iota_i\theta_{i,M}^6+\frac{1}{4}K+\frac{1}{2}\sum_{i=2}^{n}B_i^2$ with $\bar{\varepsilon}_{\Xi M}=\max\{\bar{\varepsilon}_{1,\Xi},\bar{\varepsilon}_{2,\Xi},\ldots,\bar{\varepsilon}_{n,\Xi}\}$, the design parameters ϑ_i,ζ_i and τ_i are chosen to make $\vartheta_i>\frac{1}{2},\zeta_i>0$, and $\tau_i<1$ respectively. Besides, γ_i should be selected to make $\gamma_{min}-\frac{1}{2}>0$. The vector k is chosen to make $A-kc^T$ be Hurwitz, and ensure $(A-kc^T)_{max}+1<0$.

In what follows, we discuss the system stability in two cases based on (74).

Case 1: $\dot{J}(\hat{E})<0$ In this case, according to (61), one has $\sum(\hat{E},\hat{U}^*)=0$. Since $\nabla J>0$, there exists a postive constant $\dot{\hat{E}}_{min}$ satisfying $0<\dot{\hat{E}}_{min}<\|\dot{\hat{E}}\|$. Thus, (74) changes into

$$\begin{aligned}\dot{J}_{HJB}\le&-\big(\gamma_{min}-\frac{1}{2}\big)\Big(\|\hat{E}\|+\frac{\sqrt{K}}{4(\gamma_{min}-\frac{1}{2})}\Big)^2-\Big(\alpha_2\\ &\times\dot{\hat{E}}_{min}-\beta_1\Big)\|\nabla J\|-\beta_2\|\widetilde{W}\|^4/\rho^2-\beta_3\|\widetilde{\xi}\|^2\\ &-\frac{1}{4}\sum_{i=1}^{n}\zeta_i\|\widetilde{\theta}_i\|^2+\beta_5\end{aligned} \tag{75}$$

where $\beta_5=\frac{K}{16(\gamma_{min}-\frac{1}{2})}+\beta_4+\sum_{i=1}^{n}\frac{(\vartheta_i\theta_{i,M})^2}{4(\vartheta_i-\frac{1}{2})}>0$. Provided that $\alpha_2\dot{\hat{E}}_{min}-\beta_1>0$, the following inequalities hold

$$\begin{aligned}\|\hat{E}\|&\le\sqrt{\frac{\beta_5}{\gamma_{min}-\frac{1}{2}}}+\frac{\sqrt{K}}{4(\gamma_{min}-\frac{1}{2})},\\ \|\nabla J\|&\le\beta_5/(\alpha_2\dot{\hat{E}}_{min}-\beta_1)\\ \|\widetilde{W}\|&\le\sqrt[4]{\beta_5\rho^2/\beta_2},\quad\|\widetilde{\xi}\|\le\sqrt{\beta_5/\beta_3},\quad and\\ \|\widetilde{\theta}_i\|&\le\sqrt{4\beta_5/\zeta_i},\quad i=1,\ldots,n\end{aligned}$$

Case 2: $\dot{J}(\hat{Z})\ge 0$

In this case, according to (61), one has $\sum(\hat{Z},\hat{U}^*)=1$. Add and substract $\alpha_2\nabla J(D\nabla^T\phi(\hat{E})W/2+\nabla\varepsilon/2+\widetilde{F})$ to (74), we can obtain

$$\begin{aligned}\dot{V}_{HJB}\le&-(\gamma_{min}-\frac{1}{2})\Big(\|\hat{E}\|+\frac{\sqrt{K}}{4(\gamma_{min}-\frac{1}{2})}\Big)^2\\ &+\nabla J^T(F+GU^*)+\alpha_2\nabla J^TD\nabla\varepsilon/2+\alpha_2\nabla J^T\widetilde{F}\\ &-\beta_2\|\widetilde{W}\|^4/\rho^2-\beta_3\|\widetilde{\xi}\|^2-\frac{1}{4}\sum_{i=1}^{n}\zeta_i\|\widetilde{\theta}_i\|^2+\beta_5\end{aligned} \tag{76}$$

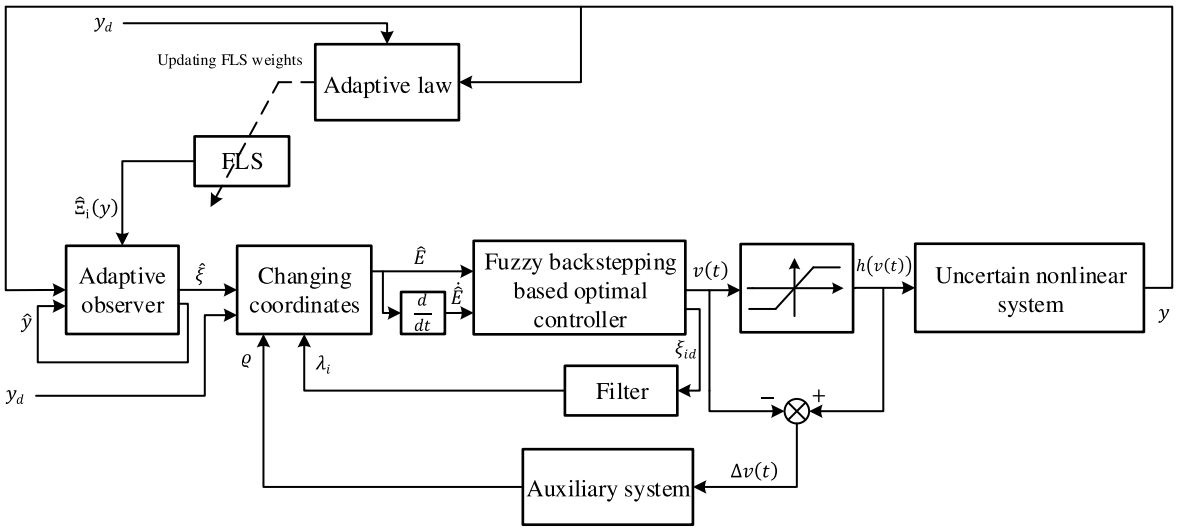

FIGURE 1. The schematic of the proposed method.

Recalling (50) and (69), and completing the squares, one obtains

$$\begin{aligned}\dot{J}_{HJB} \le & -\gamma_{min}\Big(\| \hat{E} \| + \frac{\sqrt{K}}{4(\gamma_{min}-\frac{1}{2})}\Big)^2 - \frac{1}{2}\alpha_2 \\ & \times \bar{P}_{min}\|\nabla J\|^2 - \beta_2\|\widetilde{W}\|^4/\rho^2 - \beta_3\|\widetilde{\xi}\|^2 \\ & - \sum_{i=1}^{n}\Big(\frac{1}{4}\zeta_i - \frac{4-\alpha_2}{\bar{P}_{min}}\Big)\|\widetilde{\theta}_i\|^2 + \beta_6 \end{aligned} \tag{77}$$

where $\beta_6 = \beta_5 + \frac{D_{max}^2+\varepsilon_M'^2}{4\bar{P}_{min}} > 0$, the design parameter ζ_i is chosen to make $\zeta_i > \frac{16-4\alpha_2}{\bar{P}_{min}}$. Therefore, the closed-loop system is still UUB, and the bounds satisfy

$$\begin{aligned} &\| \hat{E} \| \le \sqrt{\frac{\beta_6}{\gamma_{min}-\frac{1}{2}}} + \frac{\sqrt{K}}{4(\gamma_{min}-\frac{1}{2})}, \\ &\|\nabla J\| \le \sqrt{2\beta_6/(\alpha_2\bar{P}_{min})} \\ &\|\widetilde{W}\| \le \sqrt[4]{\beta_6\rho^2/\beta_2}, \quad \|\widetilde{\xi}\| \le \sqrt{\beta_6/\beta_3}, \quad \textit{and} \\ &\|\widetilde{\theta}_i\| \le \sqrt{\beta_6/\Big(\frac{1}{4}\zeta_i - \frac{4-\alpha_2}{\bar{P}_{min}}\Big)}, \quad i = 1, \ldots, n \end{aligned}$$

This completes the proof.

Next, we will show the boundedness of the real tracking error e_1. Denoting $\Gamma_1 = \max\Big\{\sqrt{\frac{\beta_5}{\gamma_{min}-\frac{1}{2}}} + \frac{\sqrt{K}}{4(\gamma_{min}-\frac{1}{2})}, \sqrt{\frac{\beta_6}{\gamma_{min}-\frac{1}{2}}} + \frac{\sqrt{K}}{4(\gamma_{min}-\frac{1}{2})}\Big\}$, then the following inequality holds

$$|\hat{e}_1| \le \| \hat{E} \| \le \Gamma_1 \tag{78}$$

thus

$$-\Gamma_1 \le \hat{e}_1 = \hat{y} - y_d \le \Gamma_1 \tag{79}$$

Denoting $\Gamma_2 = \max\{\sqrt{\beta_5/\beta_3}, \sqrt{\beta_6/\beta_3}\}$, then we have

$$-\Gamma_2 \le \widetilde{\xi}_1 = y - \hat{y} \le \Gamma_2 \tag{80}$$

Adding (79) with (80), one has

$$|e_1| = |y - y_d| \le \Gamma_1 + \Gamma_2 \tag{81}$$

(81) shows that the real tracking error is upper bounded.

Remark 4: It should be noted that tracking control problem for uncertain nonlinear system has been widely investigated, for example [39], [40]. Those methods also utilize backstepping method to design a stable system. The difference is that, optimality is taken into consideration in this paper. Therefore, the proposed method can not only guarantee a stable closed-loop system, but also minimize the consumption of control energy.

The overall structure of the proposed control strategy is schematized in Fig. 1.

VI. SIMULATION AND RESULTS

In order to validate the effectiveness of the proposed control strategy, in this section, a numerical example is investigated firstly, then, the missile guidance problem is examined. What' more, the proposed control strategy is compared with two observer based backstepping methods proposed in [41] and [42].

A. NUMERICAL EXAMPLE

Considering a strict-feedback nonlinear system given by

$$\begin{aligned} \dot{x}_1 &= -2x_1 + x_2 \\ \dot{x}_2 &= f_2(x_1, x_2) + g_2(x_1)u \\ y &= x_1 \end{aligned} \tag{82}$$

where $f_2(x_1, x_2) = -x_1^3 - x_2 + \frac{1}{4}x_2(\cos(2x_1 + x_1^3) + 1)^2 - \frac{x_1^2}{2x_2}$ is unknown function, and the function

$g_2(x_1) = \cos(3x_1 + x_1^3) + 2$. Assume that the state x_2 is unmearable. The constraint on input is set as $u_M = 20$.

In feedforward control design, the control parameters are selected as: $\gamma_1 = 20, \gamma_2 = 40, k_1 = 180, k_2 = 180, \vartheta_1 = 2, \vartheta_2 = 4, \zeta_1 = 2, \zeta_2 = 2, \iota_1 = 4, \iota_2 = 4, l = 10, \tau_2 = 0.01s$. The fuzzy membership functions are chosen as follows:

$$\mu_{F_{l1}}(\sigma) = \frac{1}{1 + \exp[-0.5(\sigma + 2 + l)^2]}$$
$$\mu_{F_{l2}}(\sigma) = \exp[-0.5(\sigma + 2 - l)^2]$$
$$\mu_{F_{l3}}(\sigma) = (\exp[-0.5(\sigma + 2 - l)^2])^2$$
$$\mu_{F_{l4}}(\sigma) = (\exp[-0.5(\sigma + 2 - l)^2])^3$$

where σ is input of FLS, then, $\varphi^l(y) = \prod_{i=1}^4 \mu_{F_{li}}(y) / \sum_{l=1}^4 \left(\prod_{i=1}^4 \mu_{F_{li}}(y)\right)$, $\varphi^l(y_d) = \prod_{i=1}^4 \mu_{F_{li}}(y_d) \Big) / \sum_{l=1}^4 \left(\prod_{i=1}^4 \mu_{F_{li}}(y_d)\right)$.

In feedback controller design, the cost function is choosen as

$$V = \int_t^\infty \hat{e}_1^2 + \hat{e}_2^2 + U^{*T} U^* d\tau$$

The fuzzy membership function are chosen as follows:

$$\mu_{F_l}(\hat{E}) = \exp[-0.5(\hat{e}_1 - l + 2)^2] \exp[-0.5(\hat{e}_2 - l + 3)^2]$$

then, $\phi^l(\hat{E}) = \mu_{F_l}(\hat{E}) / \sum_{l=1}^5 \mu_{F_l}(\hat{E})$. Besides, the design parameter is selected as $\alpha_1 = 6.4$.

For the comparison methods [41] and [42], to achieve almost the same tracking performance, the following control parameters: $c_1 = c_2 = 1, \rho_{12} = \rho_{22} = 0.1, \omega_1 = 10, \omega_2 = 22, \vartheta_{f1} = \vartheta_{f2} = 0.05, \gamma_{f1} = \gamma_{f2} = 0.4, H = [1, 100]^T, Q = diag[8, 200], \vartheta_W = 4, \gamma_W = 0.8$ are selected for the method in [41], while the following control parameters:$l1 = 4.02, l2 = 48, c1 = 4, c2 = 13, r1 = r2 = 0.01, a2 = 1, b1 = 2, b2 = 0.4, \lambda_1 = 1, \pi_1 = 0.2, \delta_1 = 0.06$ are selected for the method in [42].

The desired trajectory is set as $y_d = 1.2 \sin t$. The initial conditions are set as: $x(0) = [0.5, -0.5]^T$, $\varrho(0) = 0$, and all initial estimated weights are set to be zero.

Simulation results are presented in Figs. 2-8. From Fig. 2, we can see that all of the three methods can track the desired trajectory precisely. Fig. 3 shows the observer performance comparison of the three methods. It can be seen from the picture that the key state estimation error under the proposed fuzzy based observer is smaller than those under the other two methods. As the analysis above, that is important to the convergence of the real tracking error. Fig. 4 shows the trajectories of tracking error. As it shows, the tracking error under the presented method converges more faster. Additionally, we can see that the three methods achieve comparable tracking precision. However, the methods in [41] and [42] demand larger control effort than the proposed method do, which can be indicated in Fig. 5 and Fig. 6. Fig. 7 depicts the trajectories of the norms of $\hat{\theta}_1$ and $\hat{\theta}_2$. Combining that with Fig. 4, we can see that when the tracking error is large, the norms of estimated weights are also large. When the tracking error enters the steady state, the norms of the estimate weights vary in a small region. Fig. 8 shows the trajectory of $\hat{W}$. From it we can see that the estimated weights tend to converge.

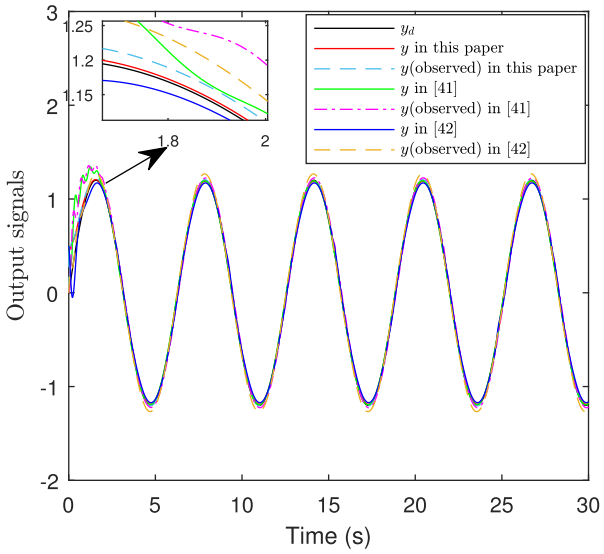

FIGURE 2. Trajectory of output signals.

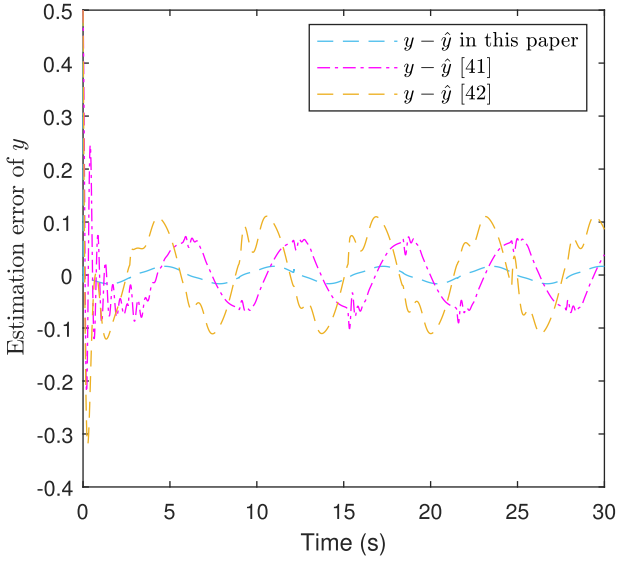

FIGURE 3. Observer performance comparison of the three methods.

B. APPLICATION TO MISSILE-TARGET INTERCEPTION SYSTEMS

In this subsection, we built mathematical model of missile-target engagement. Then, guidance simulation is conducted to validate the effectiveness of our control scheme.

Consider that a missile and a target is in engagement, as shown in Fig. 9. The velocities of the missile and target are assumed to be constant, and are denoted by V_M and V_T, respectively. Their flight path angles are denoted by γ_M and γ_T, respectively. Their lateral accelerations are denoted by a_M and a_T, respectively. The missile-target relative

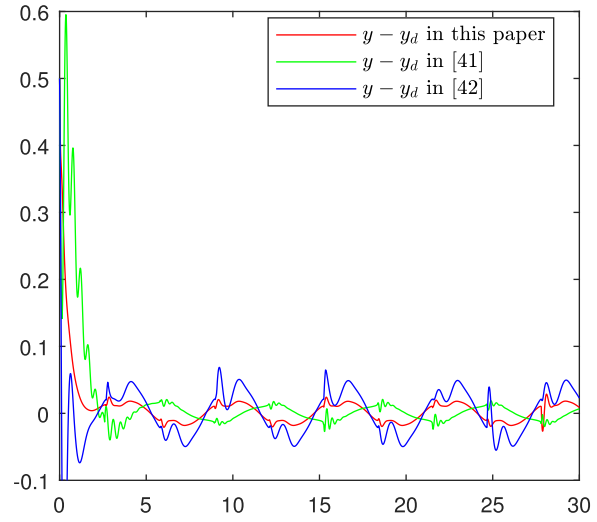

FIGURE 4. Tracking error.

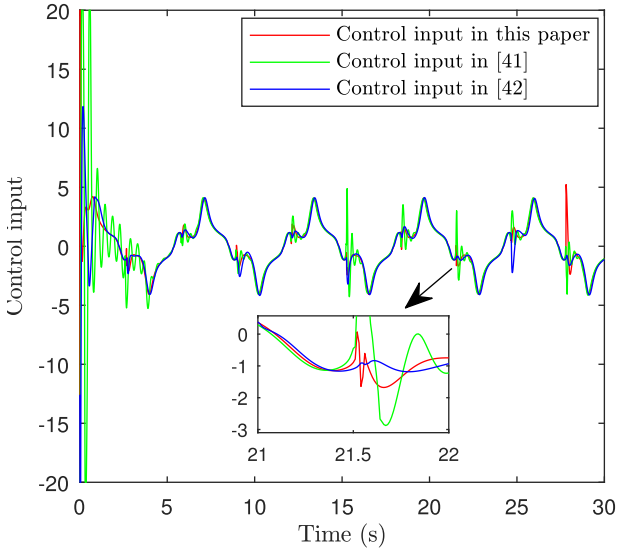

FIGURE 5. Trajectory of control input.

distance is defined as r, and LOS angle is defined as λ. Thus, nonlinear kinematic model can be described by

$$\begin{aligned}
\dot{r} &= V_T\cos(\gamma_T-\lambda)-V_M\cos(\gamma_M-\lambda)\\
r\dot{\lambda} &= V_T\sin(\gamma_T-\lambda)-V_M\sin(\gamma_M-\lambda)\\
\dot{\gamma}_M &= \frac{a_M}{V_M},\quad \dot{\gamma}_T=\frac{a_T}{V_T}\\
\dot{x}_M &= V_M\cos\gamma_M, \dot{y}_M = V_M\sin\gamma_M\\
\dot{x}_T &= V_T\cos\gamma_T, \dot{y}_T = V_T\sin\gamma_T
\end{aligned} \tag{83}$$

where (x_M, y_M) and (x_T, y_T) denotes the coordinates of the missile and the target, respectively.

Denoting $x_1 = \lambda, x_2 = \dot{\lambda}$,then, according to (83), we can obtain the following strict-feedback nonlinear system

$$\begin{aligned}
\dot{x}_1 &= x_2\\
\dot{x}_2 &= f_2(x_1,x_2)+g(x_1)a_M\\
y &= x_1
\end{aligned} \tag{84}$$

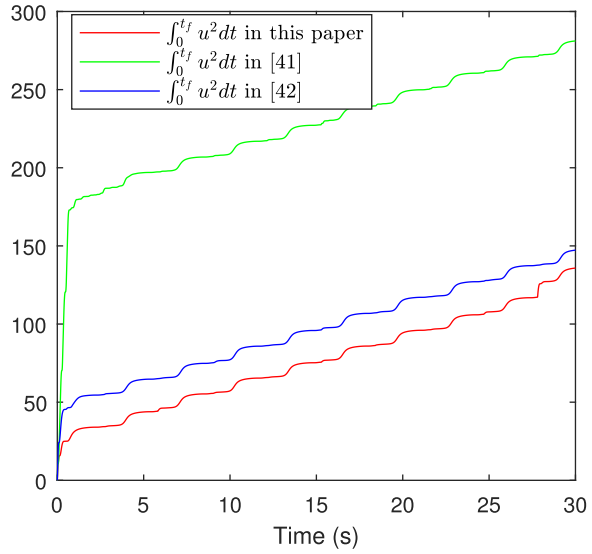

FIGURE 6. Trajectory of control cost.

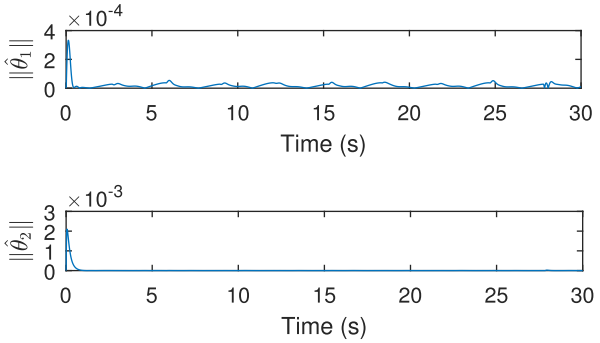

FIGURE 7. Norms of $\hat{\theta}_1$ and $\hat{\theta}_2$.

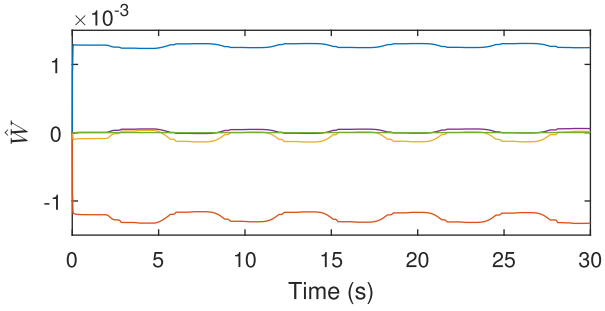

FIGURE 8. Trajectory of $\hat{W}$.

where $f_2(x_1,x_2) = -\frac{2\dot{r}}{r}x_2 + \frac{\cos(\gamma_T-x_1)}{r}a_T$,$g(x_1) = -\frac{\cos(\gamma_M-x_1)}{r}$,$u = a_M$. $f_2(x_1,x_2)$ is unknown due to the term of the acceleration of the target. Assume that x_2 can not be measured.

According to [3], a successful interception can be achieved by making the LOS rate converge to zero.

Remark 5: It should be noted that when $|\gamma_M - x_1| = \frac{\pi}{2}$, u loses control ability. Luckily, $|\gamma_M - x_1| = \frac{\pi}{2}$ is not a stable

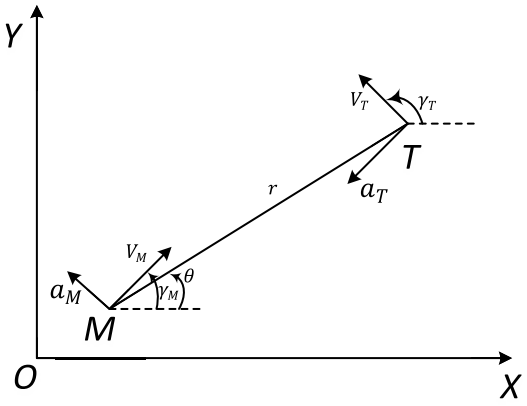

FIGURE 9. Planar engagement geometry.

equilibrium [4]. Therefore, it is feasible to choose a_M as the control input.

During simulation, the velocity of missile and target are set as $280m/s$ and $220m/s$, respectively. Assume that the target performs waving maneuvering with $a_T = 60\sin t$. Due to the physical limits of the actuator, the constraint on input is set as $u \leq 100$. Without loss of generality, the desired trajectory can be set as $y_d = 0$.

In feedforward control design, the control parameters are chosen as: $\gamma_1 = 1, \gamma_2 = 12, k_1 = 180, k_2 = 180, \vartheta_1 = 2, \vartheta_2 = 4, \zeta_1 = 4, \zeta 2 = 4, \iota_1 = 4, \iota_2 = 4, l = 20, \tau_2 = 0.01s$. The fuzzy membership functions and the cost function are as the same as those in the former subsection. In the feedback control design, the control parameters are selected as: $\alpha_1 = 12.4$.The fuzzy membership functions are as the same as those in the former subsection.

For the comparison methods [41] and [42], to achieve almost the same tracking performance, the following control parameters: $c_1 = c_2 = 1$, $\rho_{12} = \rho_{22} = 0.1$, $\omega_1 = 10$, $\omega_2 = 22$, $\vartheta_{f1} = \vartheta_{f2} = 0.05$, $\gamma_{f1} = \gamma_{f2} = 0.1$, $H = [1, 100]^T$, $Q = diag[8, 200]$, $\vartheta_W = 4$,$\gamma_W = 0.6$ are selected for the methods [41], while the following control parameters: $l1 = 2, l2 = 66, c1 = 10, c2 = 1$,$r1 = r2 = 0.01, a2 = 0.2, b1 = 0.1, b2 = 0.1, \lambda_1 = 1, \pi_1 = 0.1, \delta_1 = 0.01$ are selected for the methods [42].

Initial conditions are set as:$(x_M, y_M) = (-3000, 0)$, $(x_T, y_T) = (0, 0)$. $\gamma_M(0) = 30^o$,$\gamma_T(0) = 60^o$.

Simulation results are given in Figs. 10-16. Fig. 10 shows the flight trajectories. As we see in the picture, successful interceptions are achieved by the three methods. Fig. 11 depicts the trajectory of LOS angle. From Fig. 11, we can see that the LOS angles can converge to the desired value, and the tracking effects of the three methods are comparative. Fig. 12 shows the trajectories of LOS rate. We can observe that all of the three methods can make the LOS rate converge to zero, which is essential to lead a successful interception. Fig. 13 and Fig. 14 depict the trajectories of control input and control cost, respectively.

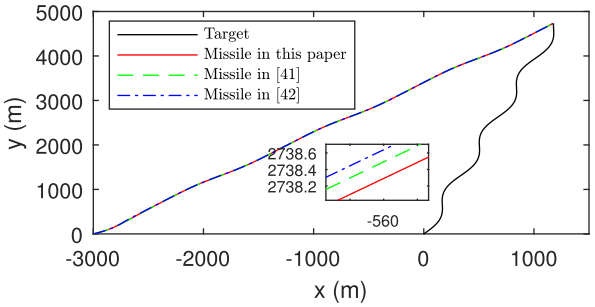

FIGURE 10. Flight trajectories.

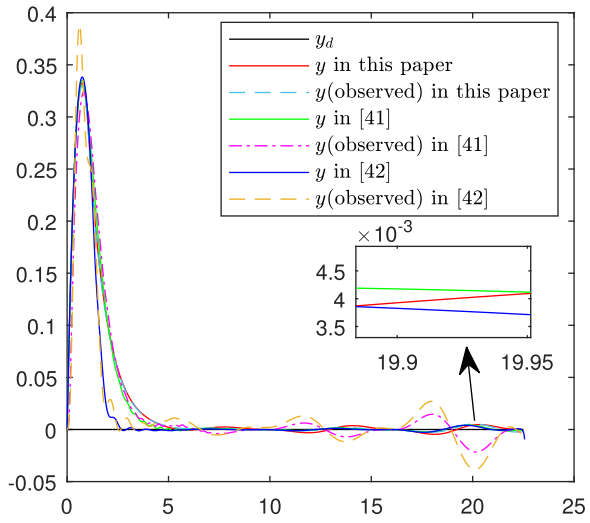

FIGURE 11. Trajectory of LOS angle.

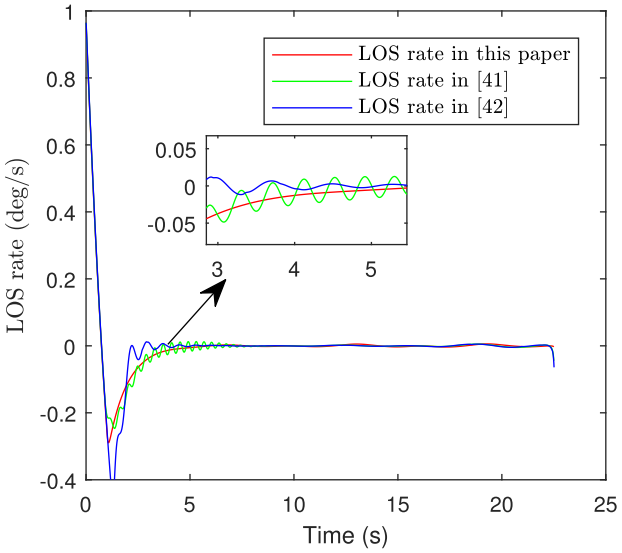

FIGURE 12. Trajectory of LOS angle rate.

The pictures indicate that the presented method still demands smaller cost of control effort. Fig. 15 depicts the trajectories of the norms of $\hat{\theta}_1$ and $\hat{\theta}_2$, and Fig. 16 depicts the trajectory of $\hat{W}$. As we see in Fig. 16, the estimated weights converge

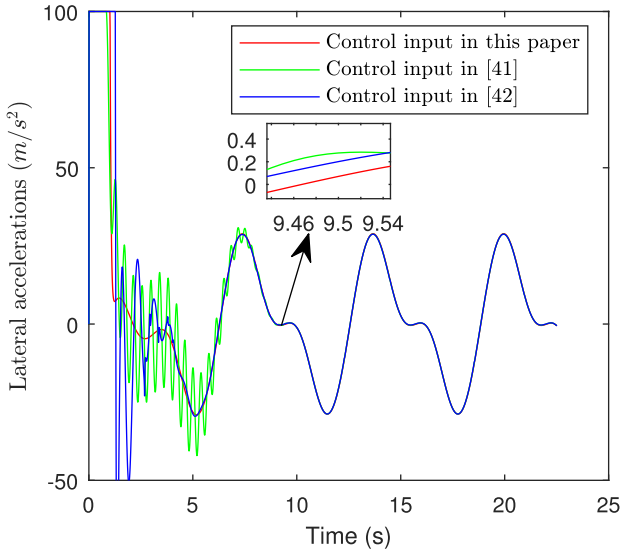

FIGURE 13. Trajectory of control input.

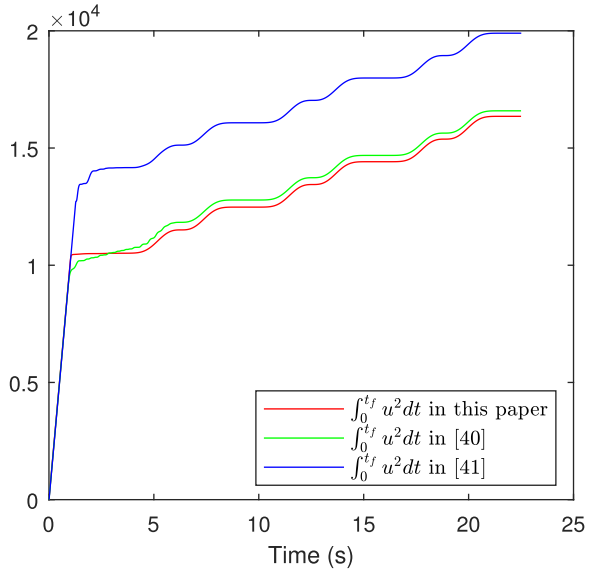

FIGURE 14. Trajectory of control cost.

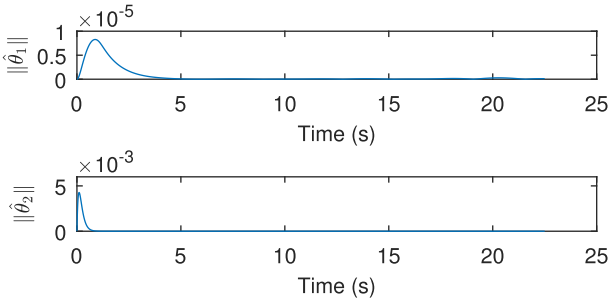

FIGURE 15. Norms of $\hat{\theta}_1$ and $\hat{\theta}_2$.

very quickly. Therefore, we can conclude that the proposed optimal tracking control scheme can obtain a comparative or even better performance at a smaller cost of control effort.

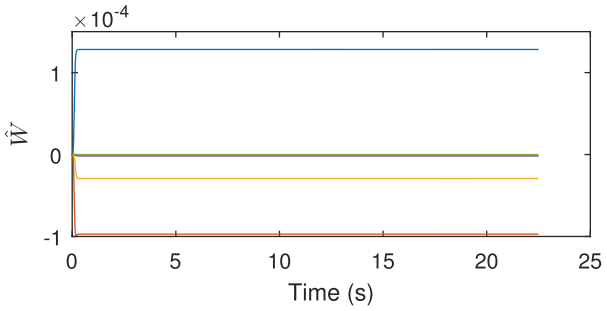

FIGURE 16. Trajectory of $\hat{W}$.

VII. CONCLUSION

In this paper, the observer-based FLS and DSC tracking control scheme for a class of strict-feedback nonlinear system is proposed in the existence of input saturation. To solve the difficulty of unmeasurable states and unknown internal dynamics, the original system is transformed into an output feedback system using FLS. Then, an observer is constructed. The estimated states is utilized in DSC design and ADP scheme. System stability is analyzed using Lyapunov theory, and all closed-loop signals are proven to be UUB. In our future work, we will focus on developing an adaptive finite-time optimal tracking control strategy based on the work in [43].

REFERENCES

[1] N. Cho and Y. Kim, "Modified pure proportional navigation guidance law for impact time control," *J. Guid., Control, Dyn.*, vol. 39, no. 4, pp. 852–872, Apr. 2016.

[2] R. Tsalik and T. Shima, "Circular impact-time guidance," *J. Guid., Control, Dyn.*, vol. 42, no. 8, pp. 1836–1847, Aug. 2019.

[3] S. R. Kumar, S. Rao, and D. Ghose, "Nonsingular terminal sliding mode guidance with impact angle constraints," *J. Guid., Control, Dyn.*, vol. 37, no. 4, pp. 1114–1130, Jul. 2014.

[4] R. Livermore and T. Shima, "Deviated Pure-Pursuit-Based optimal guidance law for imposing intercept time and angle," *J. Guid., Control, Dyn.*, vol. 41, no. 8, pp. 1807–1814, Aug. 2018.

[5] F. Sève and S. Theodoulis, "Design of an H_∞ gain-scheduled guidance scheme for a guided projectile," in *Proc. AIAA Scitech Forum*, Jan. 2019, p. 2345.

[6] I.-S. Jeon and J.-I. Lee, "Impact-Time-Control guidance law with constraints on seeker look angle," *IEEE Trans. Aerosp. Electron. Syst.*, vol. 53, no. 5, pp. 2621–2627, Oct. 2017.

[7] I. Rusnak, "Optimal guidance laws with uncertain time-of-flight," *IEEE Trans. Aerosp. Electron. Syst.*, vol. 36, no. 2, pp. 721–725, Apr. 2000.

[8] S. He and C.-H. Lee, "Optimal proportional-integral guidance with reduced sensitivity to target maneuvers," *IEEE Trans. Aerosp. Electron. Syst.*, vol. 54, no. 5, pp. 2568–2579, Oct. 2018.

[9] R. W. Morgan, H. Tharp, and T. L. Vincent, "Minimum energy guidance for aerodynamically controlled missiles," *IEEE Trans. Autom. Control*, vol. 56, no. 9, pp. 2026–2037, Sep. 2011.

[10] M. Weiss and T. Shima, "Linear quadratic optimal control-based missile guidance law with obstacle avoidance," *IEEE Trans. Aerosp. Electron. Syst.*, vol. 55, no. 1, pp. 205–214, Feb. 2019.

[11] B.-G. Park, T.-H. Kim, and M.-J. Tahk, "Range-to-go weighted optimal guidance with impact angle constraint and seeker's look angle limits," *IEEE Trans. Aerosp. Electron. Syst.*, vol. 52, no. 3, pp. 1241–1256, Jun. 2016.

[12] M. Chen, G. Tao, and B. Jiang, "Dynamic surface control using neural networks for a class of uncertain nonlinear systems with input saturation," *IEEE Trans. Neural Netw. Learn. Syst.*, vol. 26, no. 9, pp. 2086–2097, Sep. 2015.

[13] W. Wang, S. Xiong, S. Wang, S. Song, and C. Lai, "Three dimensional impact angle constrained integrated guidance and control for missiles with input saturation and actuator failure," *Aerosp. Sci. Technol.*, vol. 53, pp. 169–187, Jun. 2016.
[14] Y. Si and S. Song, "Adaptive reaching law based three-dimensional finite-time guidance law against maneuvering targets with input saturation," *Aerosp. Sci. Technol.*, vol. 70, pp. 198–210, Nov. 2017.
[15] F. Liao, Q. Luo, H. Ji, and W. Gai, "Guidance laws with input saturation and nonlinear robust H_∞ observers," *ISA Trans.*, vol. 63, pp. 20–31, Jul. 2016.
[16] G. Hexner, T. Shima, and H. Weiss, "LQC guidance law with bounded acceleration command," *IEEE Trans. Aerosp. Electron. Syst.*, vol. 44, no. 1, pp. 77–86, Jan. 2008.
[17] Q. Wei, F.-Y. Wang, D. Liu, and X. Yang, "Finite-approximation-error-based discrete-time iterative adaptive dynamic programming," *IEEE Trans. Cybern.*, vol. 44, no. 12, pp. 2820–2833, Dec. 2014.
[18] Y. Jiang and Z.-P. Jiang, "Robust adaptive dynamic programming and feedback stabilization of nonlinear systems," *IEEE Trans. Neural Netw. Learn. Syst.*, vol. 25, no. 5, pp. 882–893, May 2014.
[19] H. Zhang, L. Cui, X. Zhang, and Y. Luo, "Data-driven robust approximate optimal tracking control for unknown general nonlinear systems using adaptive dynamic programming method," *IEEE Trans. Neural Netw.*, vol. 22, no. 12, pp. 2226–2236, Dec. 2011.
[20] H. Zargarzadeh, T. Dierks, and S. Jagannathan, "Adaptive neural network-based optimal control of nonlinear continuous-time systems in strict-feedback form," *Int. J. Adapt. Control Signal Process.*, vol. 28, nos. 3–5, pp. 305–324, Mar. 2014.
[21] H. Zargarzadeh, T. Dierks, and S. Jagannathan, "Optimal adaptive control of nonlinear continuous-time systems in strict feedback form with unknown internal dynamics," in *Proc. IEEE 51st IEEE Conf. Decis. Control (CDC)*, Maui, HI, USA, Dec. 2012, pp. 4127–4132.
[22] S. Sui, S. Tong, and C. L. P. Chen, "Finite-time filter decentralized control for nonstrict-feedback nonlinear large-scale systems," *IEEE Trans. Fuzzy Syst.*, vol. 26, no. 6, pp. 3289–3300, Dec. 2018.
[23] S. Sui, C. L. P. Chen, and S. Tong, "Fuzzy adaptive finite-time control design for nontriangular stochastic nonlinear systems," *IEEE Trans. Fuzzy Syst.*, vol. 27, no. 1, pp. 172–184, Jan. 2019.
[24] S. Sui, C. L. P. Chen, and S. Tong, "Neural network filtering control design for nontriangular structure switched nonlinear systems in finite time," *IEEE Trans. Neural Netw. Learn. Syst.*, vol. 30, no. 7, pp. 2153–2162, Jul. 2019.
[25] S. Tong, Y. Li, and Y. Liu, "Observer-based adaptive neural networks control for large-scale interconnected systems with nonconstant control gains," *IEEE Trans. Neural Netw. Learn. Syst.*, early access, Apr. 20, 2020, doi: 10.1109/TNNLS.2020.2985417.
[26] W. Wang, Y. Li, and S. Tong, "Neural-Network-Based adaptive event-triggered consensus control of nonstrict-feedback nonlinear systems," *IEEE Trans. Neural Netw. Learn. Syst.*, early access, May 18, 2020, doi: 10.1109/TNNLS.2020.2991015.
[27] J. Waldmann, "Line-of-sight rate estimation and linearizing control of an imaging seeker in a tactical missile guided by proportional navigation," *IEEE Trans. Control Syst. Technol.*, vol. 10, no. 4, pp. 556–567, Jul. 2002.
[28] L. Zhang and G.-H. Yang, "Low-computation adaptive fuzzy tracking control for nonlinear systems via switching-type adaptive laws," *IEEE Trans. Fuzzy Syst.*, vol. 27, no. 10, pp. 1931–1942, Oct. 2019.
[29] L. An and G.-H. Yang, "Decentralized adaptive fuzzy secure control for nonlinear uncertain interconnected systems against intermittent DoS attacks," *IEEE Trans. Cybern.*, vol. 49, no. 3, pp. 827–838, Mar. 2019.
[30] W. Wang, S. Tong, and D. Wang, "Adaptive fuzzy containment control of nonlinear systems with unmeasurable states," *IEEE Trans. Cybern.*, vol. 49, no. 3, pp. 961–973, Mar. 2019.
[31] Y. Liu, W. Qian, Q. Lan, H. Chu, and C. Qian, "Universal finite-time observer design and adaptive frequency regulation of hydraulic turbine systems," *IET Control Theory Appl.*, vol. 10, no. 4, pp. 363–370, Feb. 2016.
[32] W. S. Park and C. K. Ryoo, "A new practical guidance law for a guided projectile," in *Proc. AIAA Guid., Navigat., Control Conf.*, Aug. 2012, p. 6249.
[33] N. Harl and S. N. Balakrishnan, "Impact time and angle guidance with sliding mode control," *IEEE Trans. Control Syst. Technol.*, vol. 20, no. 6, pp. 1436–1449, Nov. 2012.
[34] J. Sun, C. Liu, and X. Zhao, "Backstepping-based zero-sum differential games for missile-target interception systems with input and output constraints," *IET Control Theory Appl.*, vol. 12, no. 2, pp. 243–253, Jan. 2018.
[35] T. Zhang and H. Xu, "Adaptive optimal dynamic surface control of strict-feedback nonlinear systems with output constraints," *Int. J. Robust Nonlinear Control*, vol. 30, no. 5, pp. 2059–2078, Mar. 2020.
[36] C. Wen, J. Zhou, Z. Liu, and H. Su, "Robust adaptive control of uncertain nonlinear systems in the presence of input saturation and external disturbance," *IEEE Trans. Autom. Control*, vol. 56, no. 7, pp. 1672–1678, Jul. 2011.
[37] M. Krstić, P. V. Kokotovic, and I. Kanellakopoulos, *Nonlinear and Adaptive Control Design*. New York, NY, USA: Wiley, 1995.
[38] T. Dierks and S. Jagannathan, "Optimal control of affine nonlinear continuous-time systems," in *Proc. Amer. Control Conf.*, Baltimore, MD, USA, 2010, pp. 1568–1573.
[39] S. Tong and Y. Li, "Robust adaptive fuzzy backstepping output feedback tracking control for nonlinear system with dynamic uncertainties," *Sci. China Inf. Sci.*, vol. 53, no. 2, pp. 307–324, Feb. 2010.
[40] S. Tong and Y. Li, "Observer-based adaptive fuzzy backstepping control of uncertain nonlinear pure-feedback systems," *Sci. China Inf. Sci.*, vol. 57, no. 1, pp. 1–14, Jan. 2014.
[41] C. Cheng, Y. Zhang, and S. Liu, "Neural observer-based adaptive prescribed performance control for uncertain nonlinear systems with input saturation," *Neurocomputing*, vol. 370, pp. 94–103, Dec. 2019.
[42] L. Ma, G. Zong, X. Zhao, and X. Huo, "Observed-based adaptive finite-time tracking control for a class of nonstrict-feedback nonlinear systems with input saturation," *J. Franklin Inst.*, vol. 2019, no. 9, pp. 1–27, 2019.
[43] K. Sun, L. Liu, J. Qiu, and G. Feng, "Fuzzy adaptive finite-time fault-tolerant control for strict-feedback nonlinear systems," *IEEE Trans. Fuzzy Syst.*, early access, Jan. 13, 2020, doi: 10.1109/TFUZZ.2020.2965890.

WENGUANG ZHANG is currently pursuing the Ph.D. degree with the National Key Laboratory Transient Physics, Nanjing University of Science and Technology, Nanjing, China. His main research interests include adaptive dynamic programming, optimal control, and guidance systems of unmanned aerial vehicles and missiles.

WENJUN YI received the Ph.D. degree from the Nanjing University of Science and Technology.

He is currently a Professor with the National Key Laboratory Transient Physics, Nanjing University of Science and Technology. His research interests include guidance, control system design for flight vehicles, ballistic theory, and technology of new type of projectiles. He was a recipient of the Second Prize of the Chinese National Technological and Invention Award for the work on Gliding Guided Projectile and Its Engineering Application, in 2018.